

Faculdade de Engenharia da Universidade do Porto



FEUP

**Transdermal delivery of pH responsive liposomes
containing indomethacin for the treatment of
Rheumatoid Arthritis**

Miriam Machado

Dissertation for the Master Thesis in Bioengineering

Supervisor: Salette Reis
Co-Supervisor: Cláudia Nunes

18th September 2013

© Miriam Machado, 2013

Abstract

Rheumatoid Arthritis (RA) is a chronic, systemic, inflammatory autoimmune disease that targets preferentially the synovial tissue. It affects 1% of the population of the world and it is more common in women than man, in a ratio of 3:1. RA is treated recurring to several drugs such as non-steroidal anti-inflammatory drugs (NSAIDs) in the first stage of the disease which have several negative drawbacks such as low bioavailability, high clearance rates, high and frequent dosing which increase the risk of side effects.

The present work aims the development of a nanodelivery system to carry NSAIDs for the RA treatment in order to reduce the side-effects of NSAIDs. To achieve this goal four different pH responsive liposomal formulations were prepared by the thin-film method using 1,2-dipalmitoyl-sn-glycero-3-phosphoethanolamine (DPPE), cholesteryl hemisuccinate (CHEMS) and Stearylamine (SA) and indomethacin. Using DPPE and CHEMS in a ratio 7:3 multilamellar vesicles (MLV) and large unilamellar vesicles (LUV), also formulations containing DPPE, CHEMS and SA in a proportion 7:2.5:0.5 in the MLV and LUV structure. All the formulations prepared contained 1mg/mL of indomethacin. Formulations were physicochemical characterized in terms of size, zeta potential, entrapment efficiency, and morphology assessed using Transmission Electron Microscopy (TEM). Liposomes stability was evaluated throughout a month in order to study changes in size and zeta potential. LUVs possessed a size around 120 nm and MLVs 220 nm, zeta potential below -30 mV and EE of 60%. Drug release was evaluated for 48 hours at pHs 7.4 and 5.0. Also, in vitro studies using cell lines of macrophage and fibroblasts, Raw 264.7 and L929, respectively, were performed to evaluate the cytotoxic character of liposomal formulations. Finally, in vitro permeation studies were done using Franz diffusion cells to assess the permeability through the skin for a period of 8 hours.

In conclusion, it is possible to say that pH responsive liposomes were successfully prepared and shown to be promising particles for the treatment of rheumatoid arthritis.

- This page was purposely left in blank -

“Generating important negative data on a daily basis”

Unknown

- This page was purposely left in blank -

Agradecimentos

Em primeiro lugar gostaria de agradecer à Professora Salette pela oportunidade que foi poder realizar a minha dissertação sobre a sua alçada. À Cláudia por estar sempre disponível para ajudar, pelo suporte, pelas piadas e pela confiança no trabalho.

À Nini, Marina, Sofia, Catarina Alves, João Barbosa, Catarina Moura, Joana, Leandro, Daniela e Inês pela ajuda, apoio, mas acima de tudo pelo bom ambiente que criaram no laboratório o que sem dúvida aligeirava o trabalho.

À Inês e à Helena porque apesar de estarem na FEUP, estiveram sempre por perto. Aos meus afilhados, Cocas, Sardas e TJ pelo apoio e preocupação.

Ao André, Mota, Nice e Telmo agradeço pelas “distrações” sempre positivas. Pelos lanches, sorrisos, boa disposição e Costa ao longo destes últimos 6 meses.

Por último, e sim, porque o melhor fica sempre para último, quero agradecer aos meus pais e irmã porque sem eles tudo teria sido muito mais difícil.

- This page was purposely left in blank -

Index

Chapter 1 - Rheumatoid Arthritis	1
1. Pathogenesis of Rheumatoid Arthritis	2
2. Clinical Symptoms.....	3
3. Current Therapeutic Strategies	4
3.1 The NSAIDs	7
3.2 Mechanism of Action	7
3.3 Pharmacokinetics	8
3.4 NSAIDs side-effects	9
Chapter 2 - The skin	11
1. The epidermis.....	12
2. The Dermis	12
3. Skin Functions.....	13
4. Skin Permeation	15
4.1 Factors Affecting Skin Permeation.....	15
Chapter 3 - Drug Delivery Systems	17
1. Liposomes.....	18
1.1 Types of liposomes	19
1.2 pH responsive liposomes.....	22
Chapter 4- Planned Work	23
1. Methodologies and Theoretical Support	24
1.1 Dynamic Light Scattering	25
1.2 Phase Analysis Light Scattering.....	25
1.3 Phase Transition	26
1.4 Transmission Electron Microscopy	26
1.5 Drug Entrapment.....	27
1.6 Drug Release	27
1.7 In Vitro Assays	27
1.8 <i>In vitro</i> Permeation Studies	28

Chapter 5 - Materials and Methods	31
1. Preparation and Characterization of different liposomal formulations	31
1.1 Liposomes Preparation.....	31
1.2 Optimization of the methodology of liposomes preparation.....	32
1.3 Liposomes Characterization	34
1.4 Encapsulation Efficiency and Loading capacity.	35
1.5 Drug Release.....	36
1.6 Stability Assays.....	37
1.7 <i>In vitro</i> Assays	37
1.8 <i>In Vitro</i> permeation	39
1.9 Statistical Analysis.....	40
Chapter 6 - Results and Discussion	41
1. Optimization of liposomes production.....	41
2. Liposomes Characterization	41
2.1 Size.....	42
2.2 Zeta Potential	42
2.3 Encapsulation Efficiency and Loading Capacity	43
2.4 Morphology.....	44
2.5 Stability	46
2.6 Phase Transition	47
3. Release assay	48
4. <i>In vitro</i> studies.....	50
4.1 Cytotoxicity.....	50
4.2 Uptake	51
5. <i>In vitro</i> Permeation	52
Chapter 7 - Conclusions	55
Chapter 8 - Future Remarks	57
References	a
Appendix	h

List of figures

Figure 1 - Healthy Joint and Damaged Joint by the effects of rheumatoid Arthritis. [8].....	1
Figure 2 - RA inflammatory process overview. [23]	3
Figure 3 - Arachidonic Acid Cascade, adapted from [42].	7
Figure 4 - Skin Structure [75].	11
Figure 5- Functions of the epidermal barrier, adapted from [73].	14
Figure 6 - Routes of permeation through the skin [81].	15
Figure 7 - Schematic view of liposome. Cross-sectional view [92].	18
Figure 8 - Schematic illustration of liposomes based on size and number of lamellae. SUV - small unilamellar vesicle; MLV - multilamellar vesicle; LUV - Large unilamellar vesicle [97].	19
Figure 9 - The four major types of liposomes [97].	20
Figure 10 - Schematic representation of pegylated immunoliposomes where the antibody is bound directly to the liposome surface (section A) or to the distal tip of the PEG chains (C). The relative sizes are representative for a 80 nm liposome decorated with PEG2000 (PEG of molecular mass 2000 Da). When attached to the liposome surface, steric hindrance between the PEG chains in their coiled (A) as well as extended (B) conformation and the antigen- recognition site of the antibody can be expected.	21
Figure 11 - Schematic representation of the aim of the work. Indomethacin is represented by the hexagons and its location does not correspond to the location in the liposome, adapted from [123].	23
Figure 12- Example of bilayer stabilization with CHEMS and destabilization at pH 5.	24
Figure 13 - Franz diffusion cell, adapted from [140].	29
Figure 14 - Liposomes production, adapted from [124].	32
Figure 15 - Parameters used for Liposomal production optimization.	33

Figure 16- Indomethacin calibration curves for PerkinElmer Lambda45 UV/Vis spectrometer.	36
Figure 17 - Schematic representation of the viability assay, adapted from[123].	38
Figure 18 - Destabilization of lipid bilayer and hexagonal phase formation.	44
Figure 19 - TEM representative images of liposomes, (scale bar = 1 μ M). (A) MLVs 7:3 in Hepes Buffer; (B) MLVs SA in Hepes Buffer; (C) MLVs SA placebo in Acetate Buffer; (D) MLVs SA in acetate buffer; (E) LUVs 7:3 placebo in Hepes buffer; (F) LUVs 7:3 placebo in Acetate buffer; (G) LUVs 7:3 in Hepes buffer; (H) LUVs 7:3 in Acetate buffer; (I) LUVs SA in Hepes buffer and (J) LUVs SA in Acetate buffer.	45
Figure 20 - Liposomes Stability evaluated through a month. Zeta Potential and Size measurements are presented. A - MLV 7:3; B- MLV SA; C - LUV 7:3; - D- LUV SA.	47
Figure 21 - Normalized count rate vs temperature.	48
Figure 22 - <i>In vitro</i> release profiles for MLV 7:3, MLV SA, LUV 7:3 and LUV SA.	49
Figure 23 - Uptake images after 3 hours of incubation with liposomes. A - Control; B Nuclei Staining with DAPI; C - MLV 7:3 Liposomes localization. Scale bar 100 μ M.	52
Figure 24 - Permeation profiles of liposomal formulation over 8 hours. Mean and SD of two independent assays.	53
Figure 25 - Raw 264.7 viability after 24 hours of incubation with different liposome concentration, mean and standard deviation of two independent assays with 5 replica each.	h
Figure 26 - L929 viability after 24 hours of incubation with different liposome concentration, mean and standard deviation 5 replica.	i

List of tables

Table 1 - American College of Rheumatology revised criteria for classification of functional status in Rheumatoid Arthritis. [24].....	4
Table 2 - Current Treatment options for rheumatoid arthritis. Adapted from [30].	6
Table 3 -Classification of selected NSAIDs by COX-2 selectivity, chemical and pharmacokinetics properties. Adapted from [47].	9
Table 4- Skin function, adapted from [75].	12
Table 5 - Epidermis layers and their characteristics [75].	13
Table 6 - Parameters affecting Skin permeation according to their type [80].	16
Table 7 - Most common materials used in drug delivery systems [10, 32, 83-89].	17
Table 8 - Liposomes size and polydispersity. Mean and standard deviation of three independent samples. (*) Statistical significant differences, p<0.05.	42
Table 9 - Zeta Potential of the liposomal formulations (mean and standard deviation of three independent samples).	43
Table 10 - Entrapment Efficiency and Loading Capacity. Mean \pm Standard deviation of three independent samples.	43
Table 11 - Phase transition temperature and cooperativity values of MLV SA placebo, MLV 7:3 and MLV SA formulations.	48
Table 12 - IC50 values of indomethacin and liposomal formulation for Raw 264.7 and L929.....	50
Table 13 - Indomethacin concentrations after 8 hours of permeation.	53

- This page was purposely left in blank -

Abbreviations and Symbols

- μM - micro-mol/L
- ACPA - Anti-cyclic citrullinated peptide antibody
- CD4 - cluster of differentiation 4
- CHEMS - Cholesteryl Hemisuccinate
- COX - cyclooxygenase enzyme
- DAPI - 4',6-diamidino-2-phenylindole
- DLS- dynamic light scattering
- DMARDs - disease modifying anti-rheumatic drugs
- DMEM - Dulbelco's Modified Eagle Medium
- DMSO - Dimethyl Sulfoxide
- DPPE - 1,2-Dipalmitoyl-sn-glycero-3-phosphoethanolamine
- EE - encapsulation efficiency
- FBS - Fetal Bovine Serum
- IL-1, IL-6 - Interleukin 1, 6
- LC- Loading capacity
- LUV - large unilamellar vesicles
- LUV 7:3 - DPPE:CHEMS (7:3) large unilamellar vesicles
- LUV SA - DPPE:CHEMS:SA (7:2.5:0.5) large unilamellar vesicles
- MHC - Major histocompatibility complex
- MLV - multilamellar vesicles
- MLV 7:3 - DPPE:CHEMS (7:3) multilamellar vesicles
- MLV SA - DPPE:CHEMS:SA (7:2.5:0.5) multilamellar vesicles
- mM - mili-mol/L
- MTT - 3-(4,5-dimethylthiazol-2-yl)-2,5-diphenyltetrazolium bromide
- MTX - metrotrexate
- NBD - 1,2-dipalmitoyl-sn-glycero-3-phosphoethanolamine-N- (7-nitro-2-1,3-benzoxadiazol-4-yl)
- NSAIDs - nonsteroidal anti-inflammatory drugs
- PALS - Phase analysis light scattering

PEG - poly-ethylene-glycol

Pen Strep - Penicillin Streptomycin

RA - Rheumatoid Arthritis

RF - Rheumatoid Factor

SA - Stearylamine

SUV - small unilamellar vesicles

TEM - Transmission Electron Microscopy

T_m - phase transition temperature

TNF α - Tumor necrosis factor α

Chapter 1 - Rheumatoid Arthritis

Rheumatoid Arthritis (RA) is a chronic, systemic, inflammatory autoimmune disease that targets preferentially the synovial tissue. It affects 1% of the population of the world and it is more common in women than man, in a ratio of 3:1 [1-3] Besides attacking the synovial tissue, RA can affect the whole body, since it also targets organ systems such as lungs, heart and blood vessels [4] . If untreated, the inflammation of the synovial tissue leads to macrophage activation and consequent production of cytokines, which, by their side, will cause inflammation, joint swelling bone erosion and cartilage damage (Figure 1). This will result in pain, swelling, permanent joint damage and disability. Due to these, the quality of life is diminished, the risk of morbidity increases as well as the risk of premature mortality [3, 5-7] .

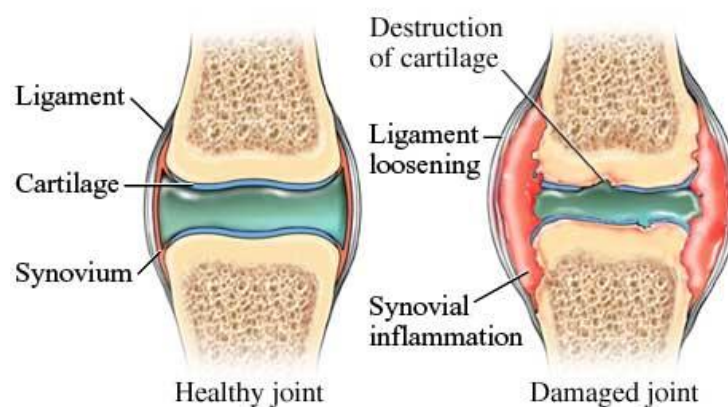


Figure 1 - Healthy Joint and Damaged Joint by the effects of rheumatoid Arthritis [8].

Since there is no cure for RA [4], the main strategies of treatment are centralized in diminishing the pain and minimizing joint damage [6, 7]. However, there are several negative drawbacks in the traditional way of RA treatment such as low bioavailability, high clearance rates, high and frequent dosing which increase the risk of side effects [9].

1. Pathogenesis of Rheumatoid Arthritis

Rheumatoid Arthritis is a complex disease in which both genetic and environmental factors play an important role in disease initiation and immunological response against the synovium [4, 10]. It occurs when genetically predisposed individuals are exposed to specific environmental risk factors. When the genetic and environmental factors interact with each other, the immune system suffers perturbations and auto-antibody-rheumatoid factor (RF), anti-cyclic citrullinated peptide antibody (ACPA) and anti-inflammatory cytokines are produced leading to arthritis inflammation [11]. Regarding genetic predisposition, it is known that the major histocompatibility complex (MHC) II is implicated in genetic risk for RA in several ethnic groups due to activation of CD4⁺ T cell [12, 13]. Other genetic risk factors are the presence of PTPN22 and PADI4 genes. The first is responsible for the survival of auto-reactive T-cells and the second influences protein citrullination [11, 14, 15]. On the other hand, the environmental factors also influence the initiation and progression of the disease. Infections [16], tobacco and over-weight [17, 18] have been shown to induce RA on individuals who have genetic predisposition [4, 16]. Smoking is undoubtedly the environmental risk factor to develop RA, however some other associations have been made. They comprise female gender, age, alcohol consumption and periodontitis [11].

A normal joint moves without pain or discomfort due to the synovial fluid that lubricates the joint allowing the movement of smooth cartilage. However, in an inflamed joint, this mechanism does not work properly. During the initial disease stages, external or self-antigens trigger immune responses that activate B-cells and T-cells. B-cells are responsible for the production of autoantibodies like RF and ACPA. T-cells activation leads to macrophage recruitment and activation and overproduction of inflammatory cytokines and consequent generalized inflammation [10, 19]. During the next stages, occurs infiltration of CD4⁺T cells, B-cells and macrophages. Macrophages are responsible for the production of proinflammatory cytokines such as tumor necrosis factor (TNF), interleukin-1 and 6 (IL-1 and IL-6) and proteases [20, 21]. After, these cytokines will activate synovial fibroblasts, creating a hypertrophied synovial lining (pannus structure) that is highly-vascularized (Figure 2). This pannus structure progressively invades and destructs cartilage and bone. Furthermore, TNF- α and IL-1 are also known to induce synovial cells to release metalloproteases that stimulate osteoclasts and subsequent bone erosion [22], figure 2. Eventually, RA will result in joint and tissue destruction and culminate in immobility and deformity.

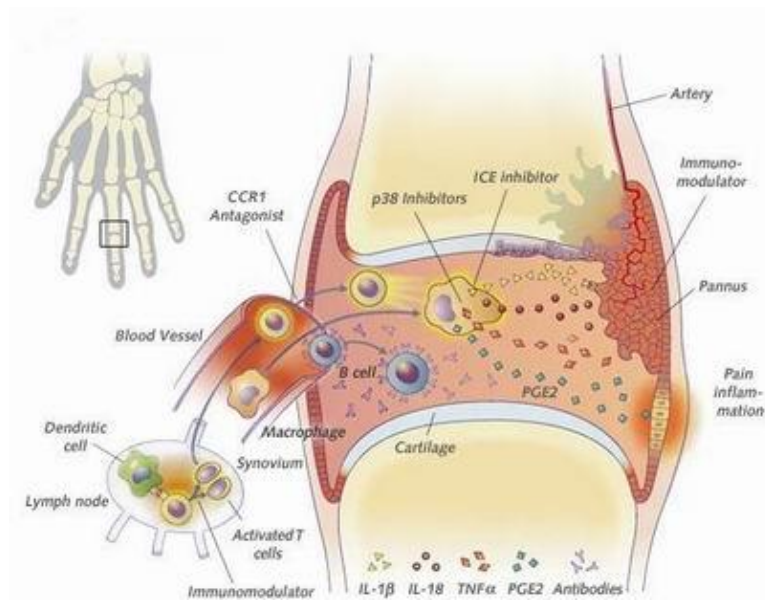


Figure 2 - RA inflammatory process overview [23].

2. Clinical Symptoms

Usually, individuals with RA present some common symptoms in the early phase of the disease such as fatigue, prolonged morning stiffness, pain that improve with activity [4]. These symptoms distinguish RA from other diseases as for example osteoarthritis.

As said previously, RA causes joints on the whole body to swell and stiffen as well as pain. According to Gaffo et al., RA involves more than five joints, on both sides of the body and attacks preferentially small joints as wrists, hands and feet joints. Regarding larger joints as knees, hips and shoulders, they are affected in later disease stage [4]. In late phases of disease progression, it occurs destructive changes in the periarticular bone, also known as bone erosion which are used to measure disease severity. In order to measure disease severity, the American College of Rheumatology produced a criteria for classification of functional status in RA (Table 1) which was approved in another studies [24].

RA can have extra articular manifestations that include subcutaneous rheumatoid nodules, anemia of chronic disease, various types of pulmonary disease, vasculitis, amyloidosis, leucopenia and eye disease [25].

Table 1 - American College of Rheumatology revised criteria for classification of functional status in Rheumatoid Arthritis¹. [24]

Class	Functional Status
Class I	Completely able to perform usual activities of daily living (self-care, vocation and avocational).
Class II	Able to perform usual self-care and vocational activities, but limited in avocational activities.
Class III	Able to perform usual self-care activities but limited in vocational and avocational activities.
Class IV	Limited in ability to perform usual self-care, vocational and avocational activities.

In 2010, the American College of Rheumatology and the European League Against Rheumatism produced a new clinical criteria for the diagnose of patients with rheumatoid Arthritis. These included history of symptom duration, a thorough joint evaluation, and at least one serologic test (RF or ACPA) positive and one acute phase response measure obtained. However these are not restrictive conditions since one person might have RA without requiring all the tests to be performed. These criteria are not only used to define if an individual as RA but also for purposes of clinical research and trial enrollment [26]. These new criteria shown to be more specific than the previous RA criteria (1987 American College of Rheumatology criteria for RA) [27, 28].

RA diagnose can be performed using several techniques. Among these, rheumatoid factor seropositivity has been the most common laboratory marker for the presence of RA, being present in 75% of the patients[29]. However RF lacks sensibility and specificity which resulted in the need of another marker. A new marker, for ACCP was found to have the same sensitivity with more selectivity [30]. Ultrasound is also used in RA diagnose, assessing soft tissue disease or detecting articular fluid collection [31]. Magnetic resonance imaging (MRI) is also used to evaluate and quantify RA manifestations [31]. The last, ultrasound and MRI are alternatives of plain radiography in early diagnosis [4].

3. Current Therapeutic Strategies

Since there is no cure for RA, the main goals of the treatment are pain relief and slowing-down disease activity. In order to accomplish these objectives, different therapies are

¹ Self-care activities include dressing, feeding, bathing, grooming and toileting. Avocational (recreational and/or leisure) and vocational (work, school, homemaking) activities are patient-desired and age- and sex-specific.

used, including therapies with nonsteroidal anti-inflammatory drugs (NSAIDs), disease modifying anti-rheumatic drugs (DMARDs), corticosteroids and biological DMARDs.

Therapeutic strategies for RA depend on the degree of synovial inflammation, articular damage and the status of articular function [32]. Treatment options for RA are summarized in Table 2.

NSAIDs are used with particular interest during the early stages of disease progression. These drugs provide pain relief and stiffness reduction due to the analgesic, anti-pyretic and anti-inflammatory effects [32-34]. NSAIDs do not change disease outcomes. The therapy using solely these drugs is not recommended since it has not been found that NSAIDs slowed RA progression. So, in long-term this therapy should be coupled with DMARD therapy [4, 34, 35]. The majority of NSAIDs act as non-selective inhibitors of the enzyme cyclooxygenase (COX), which is responsible for the production of prostaglandins (key molecules in the inflammation process) [33]. Most of the NSAIDs present a short half-life period which results in a high dosing to achieve the best therapeutic effects. The high dosage required can, however, produce several gastrointestinal side-effects, renal malfunction and increased cardiovascular risk [3, 32].

DMARDs have the characteristic of altering disease progression and hindering or reducing joint damage, being therefore effective in slowing down RA progression [33, 36]. However, DMARDs do not have any effects in pain relief so they are usually coupled with NSAIDs for better outcomes. The most common used DMARD is methotrexate (MTX) which is a metabolite that inhibits dihydrofolate reductase [10]. MTX has a rapid onset of action, high efficacy, low toxicity, ease administration and relatively low cost. Other DMARDs include hydroxychloroquine, sulfasalazine, leflunomide and gold salts [32, 35].

Glucocorticoids are a class of steroidal hormones with immunosuppressive and anti-inflammatory effects [34]. The use of these drugs may result in a significant functional improvement due to some activity in slowing-down disease progression [35]. However, glucocorticoids present unfavorable pharmacokinetic properties such as rapid clearance rates and high and frequent dosing to maintain the therapeutic levels at inflammation site which increases adverse effects [33, 37-39]. The adverse effects include insulin resistance, skin thinning, osteoporosis, hypertension, obesity and inhibition of wound repair [40]. Among glucocorticoids the most common drug is prednisone [35, 41].

Due to the advances in the knowledge of RA pathophysiology it was possible to develop a novel class of drugs to RA treatment named biological drugs/DMARDs. Biological drugs selectively block cytokines, targeting the immune response [35]. These can be divided in five categories according their effect: antitumor necrosis factor (anti-TNF), IL-1 antagonist, IL-6 antagonist, B-cell depleting agent and T-cell co-stimulation blocker [4]. However, some of these drugs are only in clinical trials testing and not yet available on the market.

Table 2 - Current Treatment options for rheumatoid arthritis. Adapted from [30].

Class	Example of agents	Mode of action	Indications	Risk and side effects
NSAIDs	Aspirin, ibuprofen, naproxen	Inhibition of COXs	Reduce acute inflammation,	Gastrointestinal disturbance and renal malfunction
	Celecoxib	Selective inhibition of COX-2	thereby decreasing pain	Lower incidence of gastrointestinal disturbance
Corticosteroids	Prednisone, Dexamethasone	Prevention of phospholipid release	Anti-inflammation	Insulin resistance, skin thinning, osteoporosis, hypertension
DMARDs	Methotrexate	Anti-metabolic activity and or extracellular adenosine release	Alteration a course of the disease	Hepatic cirrhosis, interstitial pneumonitis, myelosuppression
	Sulfasalazine	Unknown		Hypersensitivity and allergic reactions
	Hydroxychloroquine	Unknown		Retinopathy
	Leflunomide	Anti-metabolic activity		Hepatic cirrhosis, myelosuppression
	Gold salts	Unknown		Hypersensitivity reactions, nephritis
Biologic drugs	Etanercept, infliximab, adalimumab	TNF blockade	Alteration a course of the disease	Infections (tuberculosis)
	Anakinra	IL-1 receptor blockade		Infections, neutropenia
	Tocilizumab	IL-6 receptor blockade		Infections, elevated cholesterol
	Abatacept	T-cell co-stimulation blocker		Infections
	Rituximab	B- cell depletion		Infections

3.1 The NSAIDs

As said previously, NSAIDs are used to relieve the symptoms of RA. They inhibit the enzyme COX interfering with the formation of prostaglandins from arachidonic acid (Figure 3). The NSAIDs are known for the relief of local inflammation and consequent pain, stiffness, swelling and tenderness. However NSAIDs also present some toxicity which results in gastrointestinal side-effects and effects on the cardiovascular system.

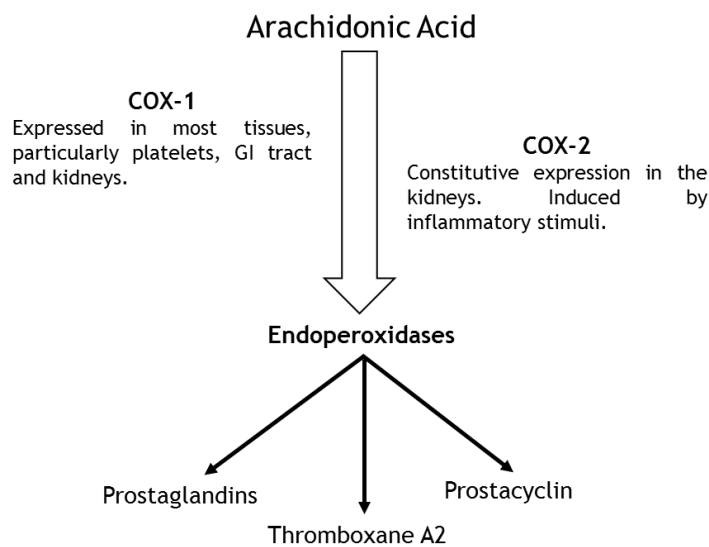


Figure 3 - Arachidonic Acid Cascade, adapted from [42].

3.2 Mechanism of Action

The mechanisms of action can be divided in three different groups according to their effects on inflammation, pain and fever. In which concerns the inflammatory effect, it is known that NSAIDs have their effect due to inhibition of cyclooxygenase enzyme [43]. In 1971, this mechanism was described by Vane and Piper. They found that NSAIDs were able to attach to the COX enzyme binding site inhibiting the ligation of arachidonic acid. Later, it was discovered that COX enzyme exists in at least two isoforms COX-1 and COX-2. In 1976 and 1991 the genes that encoded for COX-1 and COX-2, respectively, were found and characterized [44]. COX-1 enzyme is constitutively expressed throughout the body; it is responsible for the production of anti-thrombogenic prostaglandins (with cytoprotective effect on the gastric mucosa); and it is involved in the maintenance of platelet and renal functions, being therefore particularly important in the protection of gastrointestinal tract (GI) and physiological regulation of the kidney. Unlike the COX-1 gene, which is constitutively expressed in tissues like the GI mucosa and kidney, COX-2 is not normally expressed in most tissues, being induced by cytokines, growth factors and other inflammatory stimuli during periods of inflammation, to mediate pain, inflammation and fever [44-46]. Recent work has suggested that activation of endothelial cells and expression of cell adhesion molecules may interact with circulating cells and target them

to inflammation sites. NSAIDs may inhibit the expression of these cell adhesion molecules inhibiting the activation and function of inflammatory cells [47].

The inflammation will provoke the inflamed area to answer to pain stimuli that are usually painless. So, the point of action of NSAIDs in this field has to do with inflammation diminution which results in the restoration of the threshold level for pain stimuli [47, 48].

Prostaglandin E2 is responsible for triggering the hypothalamus to increase body temperature. Since NSAIDs act on the synthesis of prostaglandins they are able to reduce body temperature due to inhibition of prostaglandin E2 production [48].

3.3 Pharmacokinetics

NSAIDs can be classified in different groups according to their COX selectivity and chemical and pharmacological properties (Table 3). According to their chemical structure, NSAIDs are very similar since most of them are weak acids with amphipathic properties. However, they have some relatively significant differences in clinical outcomes due to their pharmacokinetics properties [49, 50]. Regarding their bioavailability, NSAIDs usually have high oral availability after oral administration. Also, due to the chemical structure of these molecules, they are well absorbed by the gastrointestinal tract and have low hepatic clearance [50]. One thing that needs to be taken in account is that besides the similar characteristics the behavior of all the NSAIDs, each particular type has variance in the rates of absorption [50] which result in different dosing regiments. Also, NSAIDs can be classified by their half-life period in NSAIDs with short half-life (less than six hours) and those with long half-life (Table 3). Among the NSAIDs the most common used drugs for the treatment of rheumatoid arthritis are ibuprofen and diclofenac [42].

Table 3 -Classification of selected NSAIDs by COX-2 selectivity, chemical and pharmacokinetics properties. Adapted from [47].

NSAID	COX-2 Selectivity	Chemical group	Bioavailability (%)	Half-life (h)	Volume of distribution	Clearance	Peak (h)	Protein binding (%)	Renal elimination (%)	Clinical dosage (mg/d)
Diclofenac	Non-Selective	Heteroaryl acetic acid	50-60	2	0,1-0,2 L/kg	21,0 L/h	2	>99	65	100-150
Ibuprofen	Non-Selective	Arylpropionic acid	>80	2	0,15 L/Kg	3,0-3,5 L/h	1-2	99	45-79	1200-3200
Indomethacin	Non-Selective	Indole acetic acid	80-90	4,5	0,34-1,57 L/Kg	0,195-0,229 Kg/h	4.5	97		
Ketoprofen	Non-Selective	Arylpropionic acid	90	2,1	0,1 L/kg	6,9 L/h	≤2	>99	80	200-300
Naproxen	Non-Selective	Arylpropionic acid	95	12-17	0,16 mL/min/kg	0,13 mL/min/kg	2-4	>99	95	500-1000
Celecoxib	Selective	Dyaryl-substituted pyrazole	NS	11	400 L	27,7 L/h	3	97	27	200
Eteriocoxib	Selective	Bipyridine	100	22	120 L	50 mL/min	1	92	75	60
Meloxicam	Selective	Enolic acid	89	15-20	10 L	0,4-0,5 L/h	4-5	99	59	7,5-15

3.4 NSAIDs side-effects

3.4.1 Gastrointestinal Complications

Since NSAIDs act on prostaglandins synthesis cascade, the gastrointestinal tract can suffer some damage in all its length. The most common issues related with NSAIDs therapy are some side-effects, such as dyspepsia, which take place in almost 60% of the patients [51]. Also, bleeding, endoscopic ulcers and gastric outlet obstruction may occur in patients. It is believed that NSAID therapy causes endoscopic ulcers in 10-30% of patients and serious ulcer complications in 1-2% of patients [42, 49, 51, 52]. Furthermore, poor tolerability might as well happen, which, in some cases, leads patients to discontinue [53]. In principle, the development of selective NSAIDs to COX-2 (coxibs), was expected to achieve a more effective treatment with fewer side effects, even at high doses [54, 55]. In fact, the hypothesis that at comparable

doses, NSAIDs selective to COX-2 could be as effective as traditional NSAIDs, sparing the GI mucosa, it was a premise not only attractive, but also plausible.

However, this initial simplistic interpretation that considered COX-1 as a physiological, protective enzyme and COX-2 as the enzyme responsible for inflammatory conditions is not correct and the correlation between the COX-2 selectivity of NSAIDs and their GI side effects is not always verified. In fact, some studies found that COX-2 selective-inhibitors are associated with a lower risk of ulcers and complications than the other types of NSAIDs [56-60].

Risk-factors for gastrointestinal complications include high NSAID dose, older age, *Helicobacter pylori* infection, history of ulcer or ulcer complications and concomitant NSAIDs, low-dose aspirin, anticoagulants or corticosteroids [61-63]. Usually, patients taking NSAIDs also use low-dose aspirin for cardiovascular prophylaxis, however using this combination the risk of mucosal damage increases [64, 65] and the benefits of COX-2 selective agents are eliminated [59, 60, 66].

Last but not least, in which concerns gastrointestinal complications, some drugs like diclofenac or nimesulide shown to possess hepatotoxicity as indicated by liver function tests abnormalities [67, 68].

3.4.2 Cardiovascular complications

The use of NSAIDs seems to be associated with cardiovascular complications like myocardial infarction, heart failure and hypertension [69], moreover, the risk of having cardiovascular complications increases with the exposure time [70]. It has been suggested that cardiovascular complications while taking NSAIDs may occur due to misbalance of COX-2-mediated production of pro-aggregatory thromboxane in platelets and anti-aggregatory prostaglandin I₂ in endothelial cells [46, 71, 72].

Hypertension is one of the cardiovascular complications of the use of NSAIDs. Their use can increase the blood pressure by a mean of 5mmHg. Blood pressure increment may be correlated with the increase cardiovascular events in RA [42]. Also, NSAIDs are known to cause fluid retention and systemic vasoconstriction which can worsen heart failure [42].

Cardiovascular complications are different for different NSAIDs. It is known that COX-2 inhibitors have a different behavior compared with common NSAIDs (without COX specificity). For example, there is an increased risk of thrombotic events with the use of COX-2 inhibitors and are contra-indicated in established ischemic heart disease, cerebrovascular disease and congestive heart failure [42].

However, regarding both cardiovascular and gastrointestinal complications the action of NSAIDs is not completely understood which, in a certain manner, limits the understanding of the true benefits of NSAIDs.

Chapter 2 - The skin

The skin is the largest organ of the body and it is responsible for 15% of the total body weight. The skin functions as a barrier between the inside and outside of the body protecting it against microbial invasions and water loss [73]. Besides, the skin offers protection against external physical, chemical and biological aggressions. Mainly, the skin can be divided in three layers: the epidermis, the dermis and the subcutis. The epidermis is the external layer of the skin and it is composed of layers of keratinocytes (~90 %) along with melanocytes, Langerhans and Merkel cells (~5-10 %) [74]. The dermis is the area of supportive connective tissue and contains sweat glands, hairs roots, nervous cells and fibers, blood and lymph vessels. The subcutis is the layer of loose connective tissue and fat beneath the dermis. In figure and table 4 skin structure and function are summarized.

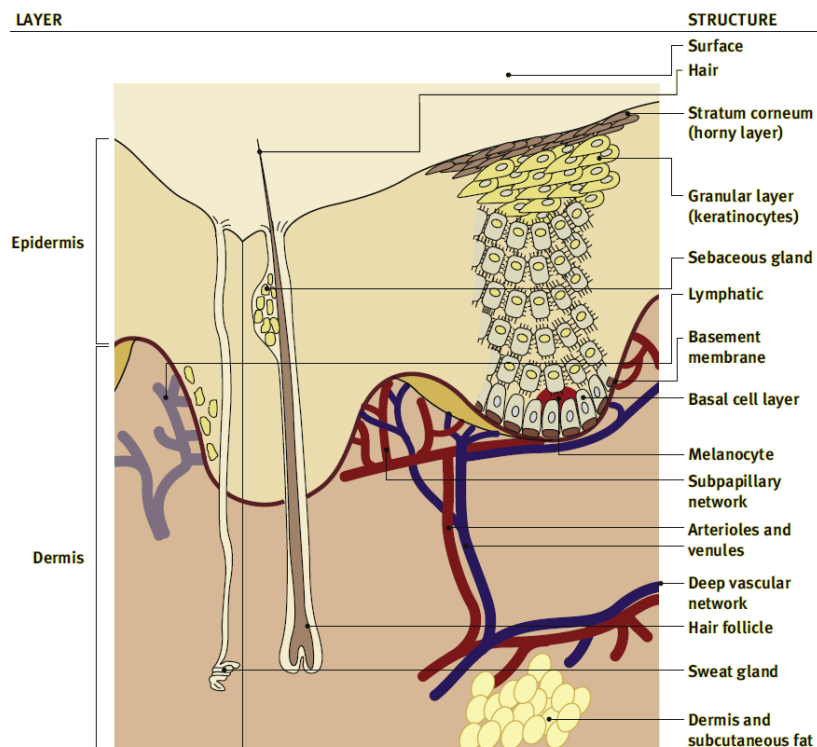


Figure 4 - Skin Structure [75].

Table 4- Skin function, adapted from [75].

Structure	Function
Hair	<ul style="list-style-type: none"> • Display and attraction; • Thermal properties.
Stratum corneum	<ul style="list-style-type: none"> • Barrier protection against unregulated loss of salt and water and entry of particles.
Granular layer	<ul style="list-style-type: none"> • Adhesion; • Cytokine production; • Keratin production; • Production of vitamin D.
Basement Membrane	<ul style="list-style-type: none"> • Adhesion of epidermis to underlying zone; • Supporting dermis.
Stratum Basale	<ul style="list-style-type: none"> • Reduplication and repair.
Melanocyte	<ul style="list-style-type: none"> • Protection against ultraviolet radiation.
Sebaceous gland	<ul style="list-style-type: none"> • Water proofing and moisturizing.
Dermis and subcutaneous fat	<ul style="list-style-type: none"> • Strength with suppleness; • Shock absorption; • Insulation.

1. The epidermis

The epidermis is, as said previously, mainly constituted by keratinocytes which synthesize keratin and are in constant motion from deeper to superficial layers. Keratinocytes regenerate through mitosis and are involved in skin repair. Also, they are known to minimize transepidermal water loss and for acting as barriers against microbial and chemical attacks [76]. The epidermis is avascular and composed of four layers: stratum basale, stratum spinosum, stratum granulosum and stratum corneum (Table 5).

2. The Dermis

The dermis is the supportive, compressible and connective tissue below the epidermis. It is predominantly composed by fibrous proteins such as elastin and collagen, produced by fibroblasts, which are responsible for elasticity and strength, respectively. It is divided in two layers: the papillary layer (thin) and the reticular layer (thick). The papillary layer interacts with the epidermis and it is composed of collagen fibers loosely attached. It contains several cells types such as fibroblasts, dermal dendrocytes and mast cells. Also, it is possible to find blood vessels and nerve endings in this layer. As it passes to the reticular layer, the

arrangement of collagen fibers changes to thicker and coarsen collagen bundles which tend to lie parallel to the skin surface. [75, 77]

Table 5 - Epidermis layers and their characteristics [75].

Epidermis layers	Characteristics
Stratum basale	<ul style="list-style-type: none"> • One cell thick; • Mainly keratinocytes in cuboidal shape; • 5-10 % melanocytes.
Stratum Spinosum	<ul style="list-style-type: none"> • Keratinocytes which start to flatten and differentiate; • Connected by desmosomes; • Langerhan cells.
Stratum granulosum	<ul style="list-style-type: none"> • Keratinocytes loose the nuclei and flatten; • Nuclei and cytoplasm appear granular; • Lipid content of the cell is discharged into the intercellular space.
Stratum corneum	<ul style="list-style-type: none"> • Superficial layer of epidermis; • Composed of cells that have migrated from the stratum granulosum (corneocytes); • Flattened and aligned morphology; • Corneocytes surrounded by keratin envelope; • Water retaining and natural physic barrier.

3. Skin Functions

The skin main function is to act as a barrier against the entrance of harmful agents and the exit of water, however, these are not the only functions associated with this organ, figure 5. Besides being a barrier against mechanical, thermal and physical injury, the skin protects the body against UV effects. Also, it is a sensory organ, helping in temperature

maintenance. Furthermore, it has role in immunological surveillance as well as in the production of vitamin D. [78]

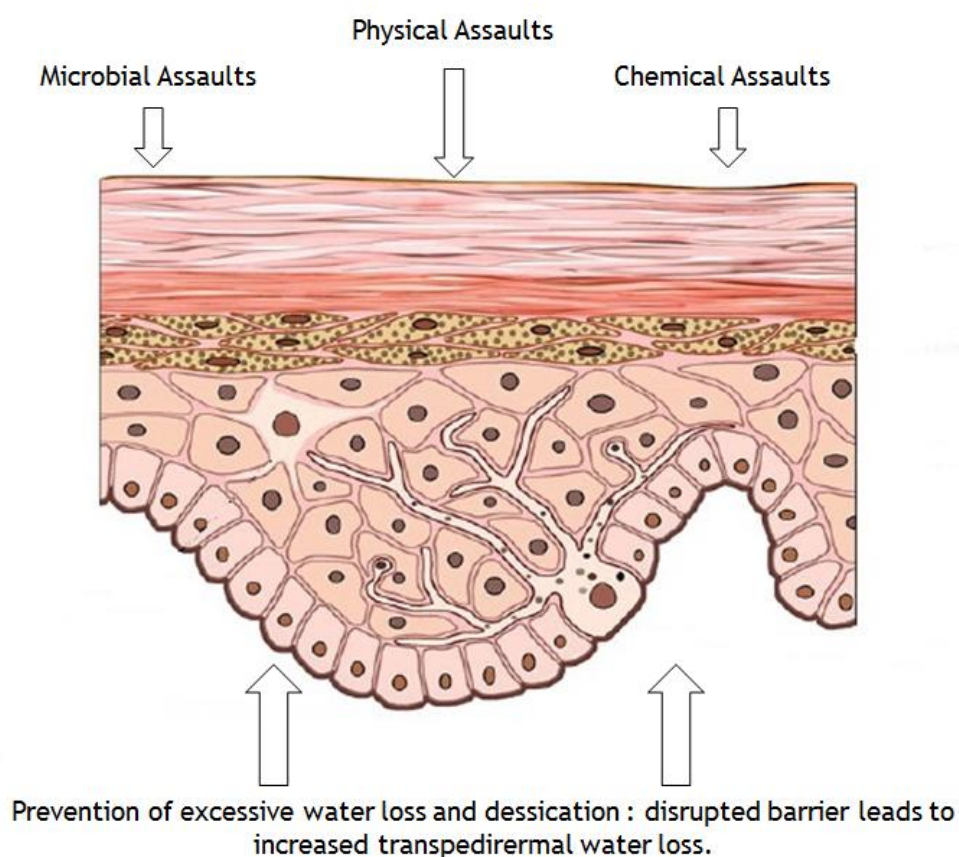


Figure 5- Functions of the epidermal barrier, adapted from [73].

Stratum corneum is the main barrier against water loss and physical assault. Due to their composition in keratinocytes arranged in a scaffold-like lattice and the existence of a lipid-rich matrix the stratum corneum acts as a robust and waterproof barrier [75].

The skin is also the first line of defense of the body. This ability is a result of the existence of epidermal Langerhans cells, transient epidermal T-cells as well as the production of anti-microbial peptides [75].

Protection against UV radiation is another skin function. The ability to protect the body against UV radiation is performed in two ways. First, the stratum corneum reflects the UV radiation which results in a diminishment of the exposure dose. Secondly, the exposition to sun results in an increase of the activity of melanocytes which transfer melanin to keratinocytes. The increase in melanin production results in a decrease in the absorption of UV radiation, since melanin absorbs the radiation. [75]

The skin is associated with thermoregulation due to changes in the blood flow at a cutaneous level and evaporation of sweat from the surface of the skin.

4. Skin Permeation

Two main routes for skin permeation have been defined: the transappendageal and the transepidermal pathway. The transappendageal route may be defined as the permeation through hair follicles and/or sebaceous glands whereas the transepidermal pathway concerns the permeation through the intact stratum corneum, figure 6. [77, 79, 80]

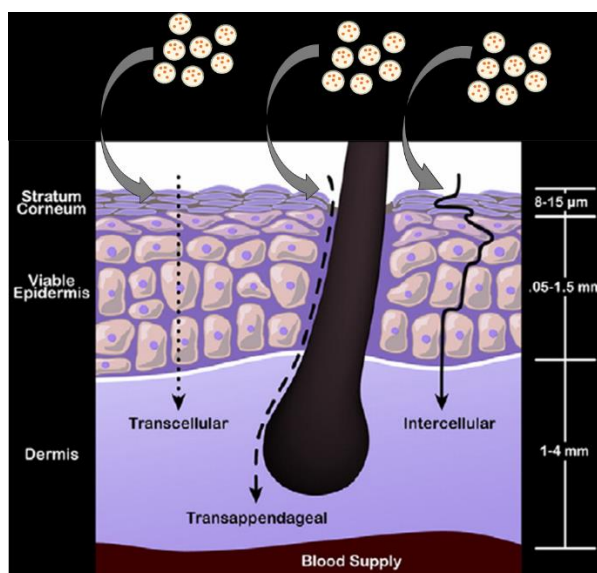


Figure 6 - Routes of permeation through the skin, adapted from [81].

The transepidermal pathway may be divided in two different subpathways: the intercellular and the transcellular pathways. In the intercellular route the molecules pass through the lipid domains of the skin, whereas on the transcellular route the molecules pass through the keratinocytes and then through the intercellular lipids. [77]

4.1 Factors Affecting Skin Permeation

Skin permeation is directly affected by the size of the molecule trying to pass through the skin. Molecules smaller than 5-7 nm can cross the skin through the intercellular route, while larger molecules (10 μm - 210 μm) cross the skin through the transappendageal pathway [80]. However, it is believed that molecules with size ranges between the 5 nm and 10 μm may cross the skin through both pathways.

Besides the importance of the size of the molecules there are some factors that have a great impact in skin permeation such as (a) location and skin conditions and the application site, (b) physicochemical characteristics of the penetrating drug and (c) physicochemical characteristics of the nanomaterial [80].

Table 6 - Parameters affecting Skin permeation according to their type [80].

<p style="text-align: center;">Location and skin conditions at application site</p>	<ul style="list-style-type: none"> • Skin integrity and regional variation; • Dimension of orifices, aqueous pores and lipidic fluid paths; • Density of appendages; • Age; • Skin type; • Sex hormones; • Dermatological and pathological conditions; • Damage; • Trauma; • Dehydration; • Skin temperature; • Environmental conditions.
<p style="text-align: center;">Physicochemical characteristics of the penetrating drug</p>	<ul style="list-style-type: none"> • Solubility; • Amount of drug; • pK_a and pH; • Oil in water partition coefficient; • Molecular weight; • Potential for binding and metabolism; • Diffusion coefficient.
<p style="text-align: center;">Physicochemical characteristics of the nanomaterial</p>	<ul style="list-style-type: none"> • Dimensions; • Shape; • Superficial properties (charge, polarity); • Solubility; • Oil in water partition coefficient.

Chapter 3 - Drug Delivery Systems

Due to the side effects of many drugs, drug delivery systems are being developed in order to achieve fewer complications. Nanoparticles are more interesting compared with microparticles due to a greater cell uptake [82]. The main objective of using drug delivery systems is the reduction of systemic side-effects and maintenance of appropriate drug concentration in the required place. Nanoparticles can be produced using different materials synthetic or natural, organic or inorganic, Table 7 summarizes some types of materials used for drug delivery systems.

Table 7 - Most common materials used in drug delivery systems [10, 32, 83-89].

Material Type	Examples
Natural Polymers	Chitosan, Gelatin, lectin, sodium alginate albumin.
Synthetic Polymers	Cellulose, poly(2-hydroxyl ethyl methacrylate), poly (N-vinyl pyrrolidone), poly (methyl methacrylate), poly (vinyl alcohol), poly (Acrylic Acid), polyacrylamide, poly (ethylene-co-vinyl acetate), PEG, poly (glycolic acid)(PLA), poly (lactide-glycolic acid)(PLGA), polycaprolactone.
Biodegradable Polymers	Poly(glycolic Acid) (PGA), PLA, PLGA, polycaprolactone.
Cyclic Oligosaccharides	Functionalized Cyclodextrin.
Magnetic Oxides	Fe ₃ O ₄ , γ- Fe ₂ O ₃ , Iron, cobalt and FeCo alloys.
Metal Oxides	TiO ₂ , ZnO-
Gold	Gold
Silicon	Porous Silicon

Also, besides the materials cited above, there are also many other nanosystems. These include liposomes and niosomes, magnetic nanoparticles, nanoshells, quantum dots, carbon nanotubes, carbon nanohorns, nanodiamonds, colloidal gold, ceramics, dendrimers, solid lipid nanoparticles, micelles and nanoemulsions [10, 32, 83, 90, 91].

The aim of any drug delivery system is to modulate the pharmacokinetics and/or tissue distribution of the drug in a beneficial way. Among the variety of delivery systems that have been devised over the years, this work will focus on liposomes. Because of the ability of liposomes to carry a wide variety of substances, their structural versatility and the innocuous nature of their components, liposomes have been studied for many different therapeutic situations. To understand how liposomes can best be used to improve the performance of the enclosed drug, some of their characteristics will be developed in the following sections.

1. Liposomes

Liposomes are small lipid bilayer vesicles that possess an aqueous core. This characteristic allows the liposomes to entrap both hydrophilic and lipophilic drugs (figure 7). They are derived from naturally occurring, biodegradable and non-toxic lipids [32] which in aqueous environment form a lipid bilayer. In the lipid bilayer, lipophilic drugs, such as dexamethasone, may be incorporated while the aqueous core may entrap the hydrophilic molecules, like diclofenac [92, 93].

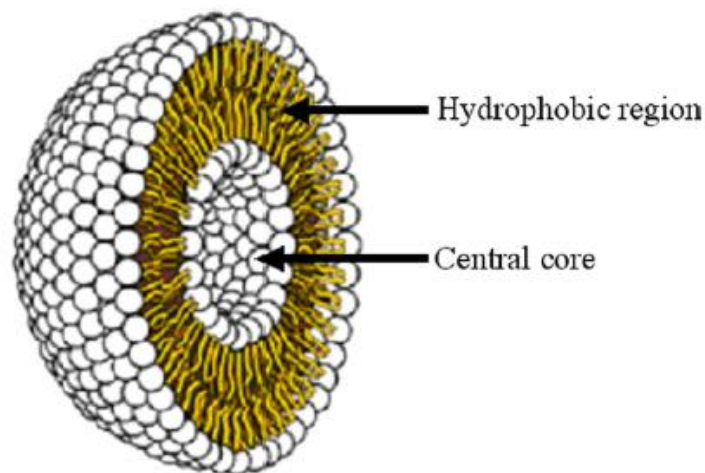


Figure 7 - Schematic view of liposome. Cross-sectional view [92].

Regarding their structure, they can be classified as multilamellar vesicles (MLV), small unilamellar vesicles (SUV) and large unilamellar vesicles (LUV) depending on their size and number of lipid bilayers (figure 8). Liposomes can have a size ranging from 30 nm to several micrometers being SUV the smallest (10-100 nm) [94]. MLV have more than one bilayer and their range in size from a few hundred nanometers to several micrometers [95, 96]. In order to obtain different types of liposomes, several lipids may be used which results in different liposome characteristics [97].

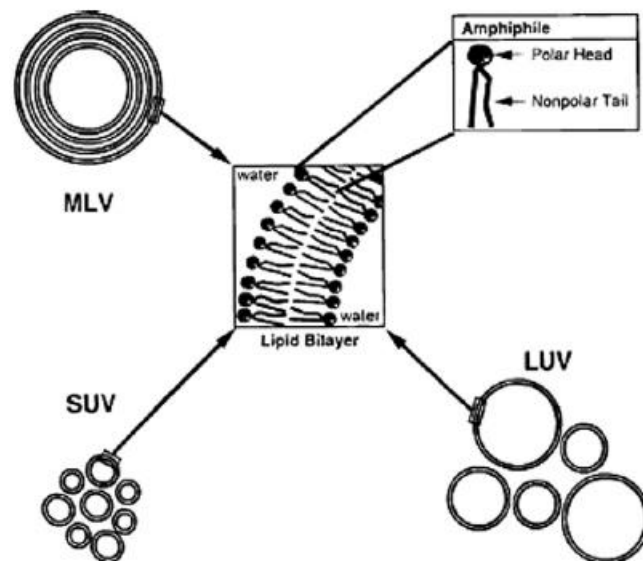


Figure 8 - Schematic illustration of liposomes based on size and number of lamellae. SUV - small unilamellar vesicle; MLV - multilamellar vesicle; LUV - Large unilamellar vesicle [97].

Liposomes have been used as formulations for poorly soluble drugs for oral or parenteral administration [98], however, it has been shown that conventional liposomes have a very high systemic plasma clearance. After injection in the body it was found that they were rapidly removed from circulation due to macrophage phagocytosis, which mainly occurred in the liver, spleen and bone marrow [99]. Inflamed tissues are characterized by enhanced vascular permeability, which allows small, long circulating drug carrier systems to extravasate at these sites via enhanced retention and permeability effect [33] which makes drug delivery systems suitable for treatment of RA.

1.1 Types of liposomes

Liposomes may be classified as conventional liposomes, cationic liposomes, stealth liposomes which increase circulating time and immunoliposomes that target specific cells and tissues (figure 9).

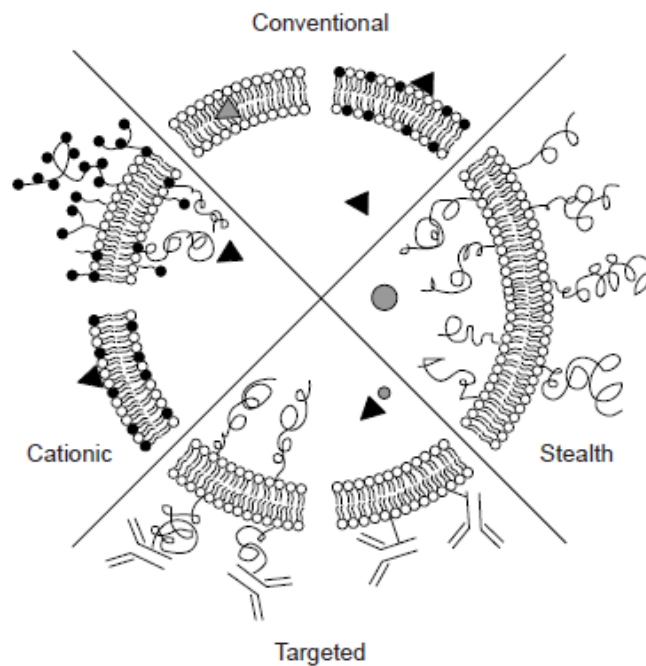


Figure 9 - The four major types of liposomes [97].

1.1.1 Conventional Liposomes

Conventional liposomes are composed by lipid or lipid mixtures and are the simplest liposomes to produce. However, since they are only composed by lipids they have high clearance rates. When in circulation, conventional liposomes are rapidly coated with plasma proteins which results in phagocytosis by the reticuloendothelial system cells. Liver, spleen and bone marrow are the principal phagocytosis sites due to their content in those cell types [97, 99]. Usually rapid clearance is not desired and liposome modification may be required to achieve better results.

1.1.2 Long circulating “stealth” liposomes

In order to prolong the half-life period of liposomes, some molecules, such as polyethylene-glycol (PEG), have been incorporated within the phospholipid bilayer of conventional liposomes. Hydrophilic surfaces are known for impeding plasma protein adsorption due to steric stabilization of the liposome surface. In the case of PEG, steric stabilization occurs due to hydration of surface PEG groups that will prevent interaction with proteins and biological molecules, which results in an increased circulation period [100]. Several studies shown that the attachment of PEG on nanoparticles surface (PEGylation) resulted in a smaller rate of elimination by the liver and a higher accumulation in inflamed synovium, when compared to non-PEGylated nanoparticles [86, 101, 102]. This means, that PEGylation of liposomes will increase the bioavailability of drugs, allowing a slow release of the drug which reduces side-effects and drug toxicity [103-105].

Stealth liposomes are also able to cross vascular walls in inflamed sites due to the enhanced permeability, characteristic of this tissues. The enhanced permeability conjugated with PEG characteristics allows liposomes to extravasate and act in these locals [94].

1.1.3 Cationic Liposomes

Cationic liposomes are usually used as delivery systems for genetic materials. Since DNA has a negative charge, the positive charge of the liposome will neutralize DNA chains which results in a higher compact structure [106-109]. The DNA-lipid complex will promote cellular internalization and protection, and expression of the plasmid [94].

1.1.4 Immunoliposomes

Immunoliposomes are able to target and recognize specific cells or organs due to the presence of targeting vectors on their surface. Examples of targeting vectors include proteins, peptides and small molecules such as, for example, folate which was used to target folate-receptor, which is overexpressed in tumor and inflamed macrophages [110-112].

PEGylated liposomes have minimal affinity to cells being a platform to design targeted liposomes. Several coupling strategies exist to attach proteins to phospholipids or to PEGylated phospholipids while their biological activity is maintained (Figure 10). These strategies include covalent coupling to phospholipids (Figure 10, A and B) or coupling to the terminus of PEG chains (Figure 10, C) [98]. The main problem regarding the coupling of proteins to the liposome surface is that PEG may have a shielding effect that may inhibit the interaction between the ligand and its receptor [113]. However, using the coupling to PEG technique, it was found that target binding efficiency increased by a factor of two to three [114, 115].

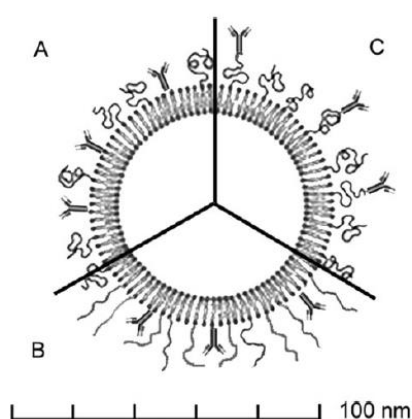


Figure 10 - Schematic representation of pegylated immunoliposomes where the antibody is bound directly to the liposome surface (section A) or to the distal tip of the PEG chains (C). The relative sizes are representative for a 80 nm liposome decorated with PEG2000 (PEG of molecular mass 2000 Da). When attached to the liposome surface, steric hindrance between the PEG chains in their coiled (A) as well as extended (B) conformation and the antigen-recognition site of the antibody can be expected.

1.2 pH responsive liposomes

Inflammation causes two major pathophysiological changes: hypoxia and acidosis which, on their turn, result in a pH decrease in the inflamed site [116]. In order to use this characteristic of inflamed tissues, liposomes with pH responsiveness have been developed. These liposomes possess the ability to release their content in an environment with decreased pH. In order to obtain liposomes with these characteristics it is needed a destabilization of the liposomal membrane. Liposomal membrane destabilization may be induced by the bound of amphiphilic peptides that adopt an α -helical conformation in an acidic environment [117] or by the use of cationic and ionizable anionic lipids [118]. Therefore, pH sensitive liposomes can be produced by a mixture of a cationic lipid, such as dioleoylphosphatidylethanolamine (DOPE), and an ionizable anionic lipid such as cholesteryl hemisuccinate (CHEMS). When at elevated pH, CHEMS stabilizes the cationic lipid in its bilayer organization. However, as the pH decreases and gets near or the pKa of CHEMS, this molecule becomes to lose its charge leading to the destabilization of the liposomes by membrane inversion, membrane fusion, and the release of entrapped substances into liposome surrounding space [119, 120]. This methodology may be applied both to conventional and PEGylated liposomes [121].

Chapter 4- Planned Work

Taking in account what has been said about RA, skin and liposomes, pH responsive liposomes were designed. Three main characteristics had to be taken in account to achieve the best performance which concerned size specifications, utilization of a formulation that at pH 7.4 is stable and at pH 5 is unstable and the ability to entrap indomethacin. Size specifications appear as a consequence of both transdermal drug delivery and uptake in inflamed locations. In order to pass through the blood vessels and to use the enhanced permeability, liposomes should have between 200 - 800 nm. [122] The main objective of this work was to produce liposomes, MLVs or LUVs containing indomethacin, with the ability to cross the skin and that at pH 5, in inflamed sites, are able to release the entrapped indomethacin, figure 11.

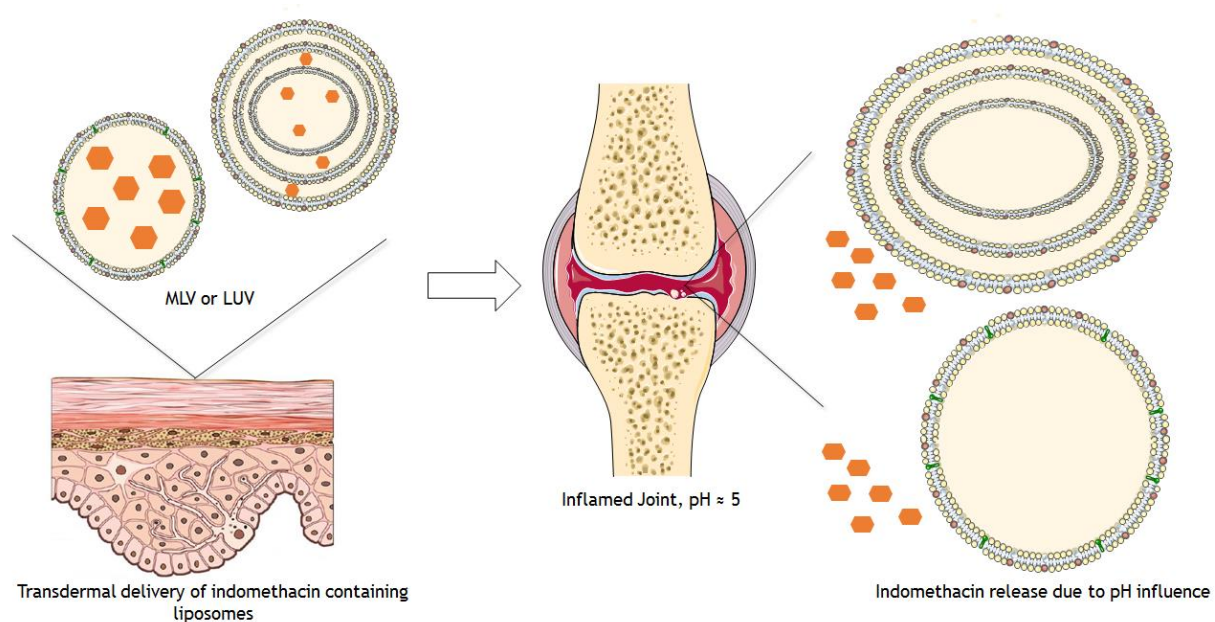


Figure 11 - Schematic representation of the aim of the work. Indomethacin is represented by the hexagons and its location does not correspond to the location in the liposome, adapted from [123].

In this work, three different lipids were used to produce different liposomal formulations. They comprised 1,2-dipalmitoyl-sn-glycero-3-phosphoethanolamine (DPPE), CHEMS and Stearylamine (SA). DPPE possesses a conic geometry since it contains a smaller polar head group compared to the phospholipid tail. CHEMS act as a bilayer stabilizer at pH

7.4. On the other hand, SA was added due to the possibility of electrostatic interactions with indomethacin at pH 7.4, which may induce an increase in the amount of encapsulated drug. When the pH lowers, occurs a destabilization between CHEMS, SA and DPPE which results in bilayer destabilization and consequent drug release, Figure 12. [124]

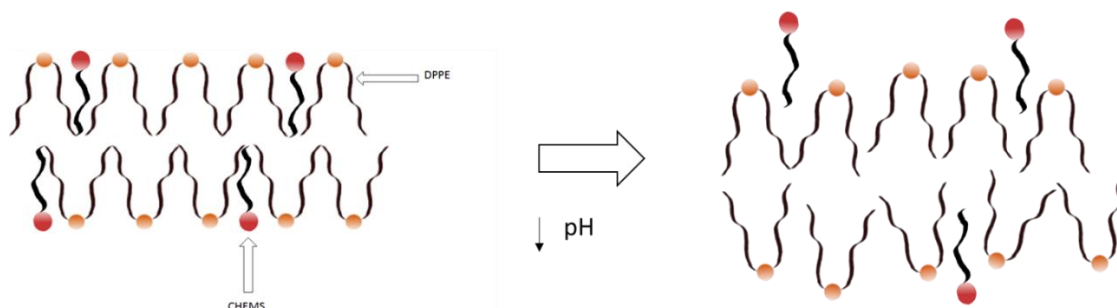


Figure 12- Example of bilayer stabilization with CHEMS and destabilization at pH 5.

Indomethacin is a non-steroid anti-inflammatory and anti-pyretic agent with chemical formula $C_{19}H_{16}NO_4Cl$. This drug is rapidly cleared from the plasma having a half-life of 0.3 to 4 hours [125, 126]. Due to its anti-inflammatory and anti-pyretic properties, indomethacin is used to treat several conditions such as rheumatoid arthritis, ankylosing spondylitis, osteoarthritis among others. [127]

As the majority of NSAIDs, indomethacin presents several major side-effects such as gastro-intestinal complications, cardiovascular effects as well as platelet aggregation inhibition. Liposomes containing indomethacin were produced in an attempt to reduce the side-effects of this drug.

Liposomes were prepared by the lipidic film hydration which will be described in the next chapter. After their production, they were physically characterized and their interaction with macrophage and fibroblasts evaluated. Also, *in vitro* permeation skin studies were performed using Franz cells. In this chapter, a brief description of the techniques used to characterize the liposomes and their theoretical support will be presented.

1. Methodologies and Theoretical Support

During the development of this work several techniques were employed in an attempt to understand liposomes physicochemical characteristics. These included size and zeta potential measurements, phase transition (T_m), morphology assessment, encapsulation efficiency (EE) and loading capacity (LC). These characteristics were evaluated using different apparatus. Size and zeta potential were measured using Dynamic Light Scattering (DLS) and Phase Analysis Light Scattering (PALS). T_m was evaluated using DLS and morphology was assessed using Transmission Electron Microscopy (TEM). EE and LC were both analyzed using spectrophotometric analysis.

Regarding their interaction with cells two separate assays were performed cytotoxicity, using a MTT assay and uptake using a staining protocol in Raw 264.7, a macrophage cell line. Also, in pursue of scientific curiosity, preliminary assays on a fibroblast cell line, L929 were also done. Last but not least, an *in vitro* permeation skin study was performed to assess liposome ability to pass through the skin.

1.1 Dynamic Light Scattering

The DLS technique was used to measure size. When in suspension, colloidal sized particles undergo random movement (Brownian motion) colliding with the driven molecules of the liquid. With the increase in particle size the particle will have a slower Brownian motion, so, smaller particles move more rapidly. The scattered light intensity will fluctuate in time and give information about the diffusion coefficient of the particles. In this apparatus, a light beam, with a fixed wavelength λ , passes through a polarizer to define the polarization and the incident beam passes in the sample where it suffers scattering. Smaller particles will suffer fluctuations in the intensity more rapidly than the larger particles [128]. After incidence on the sample, the scattered light will be detected and recorded on the photomultiplier and using a mathematical approximation, particles size is determined.

1.2 Phase Analysis Light Scattering

PALS is a technique that during this work was used to assess Zeta Potential. The zeta potential is a measure of a particle surface charge. Zeta potential is correlated with stability of a formulation, if the liposome suspension has a charge of 30 mV in modulus, the suspension is stable and will not form molecules aggregates due to particles repulsion [129].

In zeta potential measurements, an electric field is applied on the suspension and charged particles move towards the opposite charged electrode. At equilibrium, particles move at a constant velocity which is measured using PALS. Particles speed depends on the strength of the electric field or voltage gradient, dielectric constant and viscosity of the medium, and zeta potential. The zeta potential is then determined using the well-known Henry's equation.

As said previously, PALS technique is applied to measure particles velocity. This technique uses phase shifts measurements to determine particles velocity: when light is scattered by a moving particle, its phase shifts in proportion to their velocity. The phase shift is then compared with a reference beam and particles velocity calculated.

1.3 Phase Transition

Phase transition temperature, T_m , is the temperature of change from the gel phase of the lipid bilayer to its liquid-crystalline phase. [130] The dynamic light scattering (DLS) exploiting the count rate is a reliable, simple and reproducible technique to determinate the T_m [131]. The alteration in the measured scattering intensity reflects changes in the optical properties of the material.

Thus, discontinuity in the mean count rate (average number of photons detected per second) as the temperature changes, corresponds to an alteration in the optical properties of the material studied (i.e. transition from initial state to another one) (Michel et al., 2006). Data as the normalized mean count rate versus temperature were collected and fitted using equation 1.

$$r_s = r_{s1} + p_1 T + \frac{r_{s2} - r_{s1} + p_2 T - p_1 T}{1 + 10^{B(1/T - 1/T_m)}} \quad (1)$$

where r_s is the average count rate, T is the temperature ($^{\circ}\text{C}$), p_1 and p_2 correspond to the slopes of the straight lines at the beginning and at the end of the plot, and r_{s1} and r_{s2} are the respective count rate intercepting values at the y-axis. From the experimental data displayed, it was possible to calculate the cooperativity (B) and the midpoint of the phase transition, which corresponds to the T_m . The T_m was calculated from the slope and the inflection point of the data fitted to sigmoid curves of count rate (r_s) versus temperature (T). [131]

1.4 Transmission Electron Microscopy

In TEM a high-energy electron beam is focused on the sample to achieve an image or diffraction pattern of the specimen. When a high-energy electron beam hits a thin sample, electrons suffer scattering producing several secondary signals which characterize the interactions taking place. Scattered electrons are nonuniformly distributed and this non-uniform distribution contains the structural and chemical information about the sample. The information obtained can then be viewed in two ways (a) angular distribution which is correlated with diffraction pattern and (b) special distribution of scattering which generates a contrast image of the sample. [132]

TEM microscope is composed of an optical column where the electrons are generated, electromagnetic lenses, the sample and an observation systems. Also, several apertures exist to collimate the electron beam onto the sample. TEM is a technique that allows to study morphology at a nanoscale level, which possibilities the study of specimen structure. [132]

1.5 Drug Entrapment

EE and LC are useful parameters used to evaluate liposomes as drug delivery systems. EE corresponds to the ration between the amount of drug encapsulated in the liposome and the total amount of the drug added, Equation 1, whereas LC correlates the amount of drug in the liposome with the lipid content Equation 2.

$$\%EE = \frac{\text{Amount of drug in the liposome (mg)}}{\text{Total amount of drug (mg)}} \times 100 \quad (2)$$

$$\%LC = \frac{\text{Amount of drug in the liposome (mg)}}{\text{Amount of lipid (mg)}} \times 100 \quad (3)$$

1.6 Drug Release

Drug release of pharmaceutical nanoparticle systems greatly influence their biological effect. *In vitro* release profiles are widely used to evaluate interactions between drug and lipids and their influence in the release rates and mechanisms of drug release. [133] In this experiment, the technique used to assess drug release patterns was the dialysis bag diffusion technique.

The amount of indomethacin presented at each time point was calculated based on Equation 3, which correlates the amount of indomethacin present after the incubation period with the amount of indomethacin initially placed.

$$\%Drug\ release = \frac{\text{Amount of indomethacin}}{\text{Total amount of indomethacin}} \quad (4)$$

1.7 In Vitro Assays

It is known that in inflamed sites, like arthritic joints, macrophages are present and are the main responsables for the inflammation process. In order to evaluate their response to these formulations, a macrophage cell line was used. The mouse monocyte/macrophage RAW 264.7 cell line was derived from a tumor developing in a BAB/14 mouse, 30 years ago [134].

Also, a fibroblast cell line, L929, from mouse, was used in preliminary assays to evaluate formulations cytotoxicity and to compare cytotoxicity in macrophage against fibroblasts.

1.7.1 Cytotoxicity

MTT (3-(4,5-Dimethylthiazol-2-yl)-2,5-diphenyltetrazolium bromide), figure sdf, is a yellow tetrazole reduced in the cells to purple formazan crystals by the activity of the mitochondria. The amount of formazan produced is proportional to the number of living cells and it can be quantified by absorbance measurements in the range 550-600 nm.[135] Since MTT is a rapid, convenient and economical assay it has been used widely to assess cell viability. However, there are some factors that have to be taken in account when performing an MTT assay, they comprise (a) cell density, (b) culture medium, (c) optimal concentration and exposure time for MTT among others. [136]

Also, to evaluate the effect of drugs, several drug concentrations should be tested and drug exposure times. Moreover, it is important to have controls in order to establish relation between the different concentrations and exposure times. [135]

1.7.2 Uptake

Uptake was assessed through nuclei, cell membrane and liposomes. Nuclei staining was done using 4',6-diamidino-2-phenylindole (DAPI) while for liposomes, 1,2-dipalmitoyl-sn-glycero-3-phosphoethanolamine-N-(7-nitro-2-1,3-benzoxadiazol-4-yl), NBD, was used.

DAPI is a blue dye that specifically binds cells nuclei and is excited at 358 nm. NBD is a lipid with a group that in a hydrophobic environment becomes fluorescent which allowed the staining of liposomes. [137]

1.8 *In vitro* Permeation Studies

In vitro permeation studies were carried out using Franz cell diffusion cells. These are the most common type of diffusion cells principally due to the low cost, ability to study semisolid formulations and good simulation for *in vivo* performance [138]. Porcine skin was placed between the diffusion compartments of the diffusion cell, since it is the most similar to the human's skin and also presents a permeability rate similar to the human skin. [139]

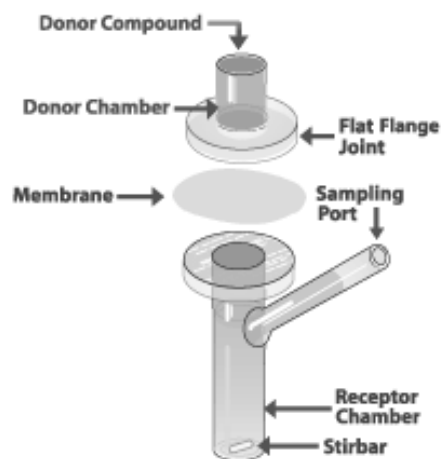


Figure 13 - Franz diffusion cell, adapted from [140].

In the donor side of the diffusion cell was placed the formulation, figure 13, above the skin, whereas on the receptor side, figure 13, below the skin, the diffusion cell contained an isotonic saline solution or a buffer and, in this case, a cosolvent to allow indomethacin solubilization. The amount of drug in the receptor side may be evaluated through several techniques such as chromatography, or spectroscopy, however in this case UV/Vis. spectroscopy was the chosen technique to analyze the amount of drug [138].

- This page was purposely left in blank -

Chapter 5 - Materials and Methods

1. Preparation and Characterization of different liposomal formulations

The steps towards liposomes production until the final formulations are described below. In the end, four liposomal formulations and their respective placebos were prepared DPPE/CHEMS (7:3) and DPPE/CHEMS/SA (7:2.5:0.5) in their MLV and LUV structure.

1.1 Liposomes Preparation

Liposomes were prepared by the extrusion film method. Firstly, MLVs were prepared. The specified amount lipids was dissolved in a solution of methanol: chloroform (3:1), from Fisher and Atom Scientific respectively, in a round-bottom flask. The suspension was then placed in a rotary-evaporator, under a stream of nitrogen, for 40 minutes at 42 °C, in order to evaporate the solvent and to allow uniform film formation. After complete solvent evaporation, an adequate volume of HEPES Buffer, pH 7.4, was added and the suspension vortexed for at least 15 min or until complete film dissolution. In order to form LUVs, the liposomal suspension was extruded. The extrusion process allowed the formation of liposomes with desired size due to pressure applied in the extrusion system, filter pore size and temperature. The suspension content was placed inside the extrusion system, and passed three times through a 600 nm polycarbonate filter, Whatman, and ten times through a 200 nm polycarbonate filter, Whatman, at 65 °C (temperature above the main phase transition of the liposomes). Figure 14 schematically exemplifies the process for liposomes production.

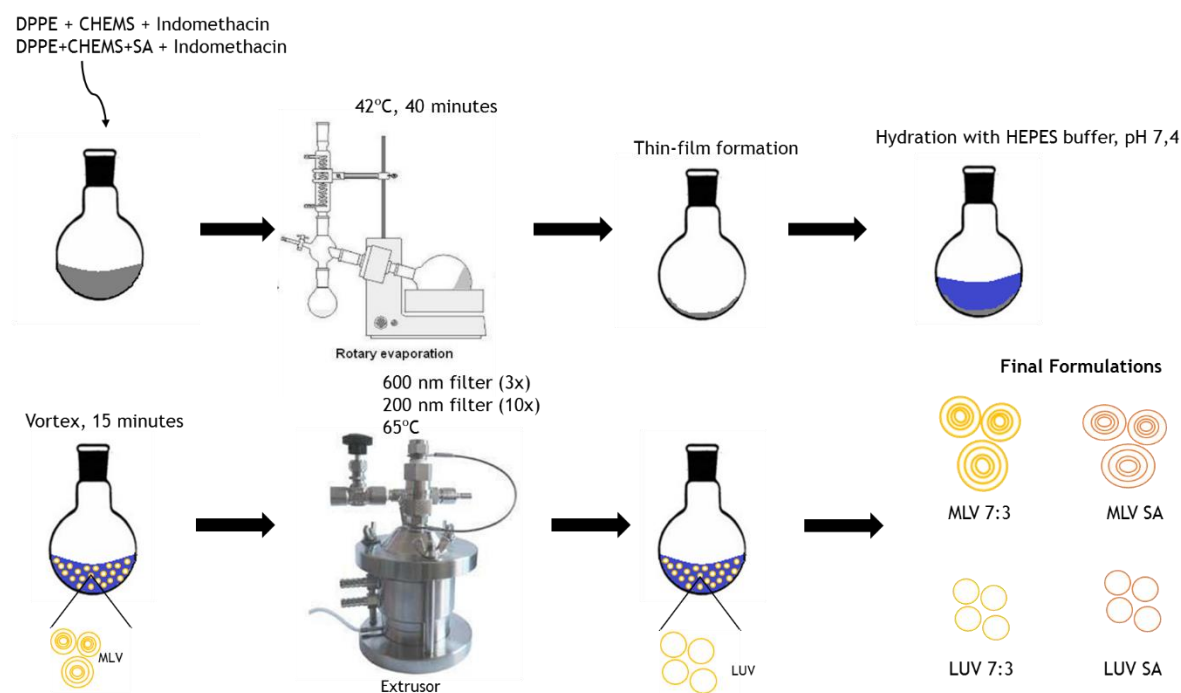


Figure 14 - Liposomes production, adapted from [124].

1.2 Optimization of the methodology of liposomes preparation

The first step towards process optimization was the use different lipid concentrations 5 mM and 15 mM. Secondly, the amount of indomethacin in the formulation was altered to increase liposomes EE.

Also, several formulations containing different lipids were produced. This formulations were DPPE:CHEMS (7:3), the base formulation, DPPE:CHEMS:SA in different proportions (7:2.5:0.5 and 7:2:1) and DPPE:SA also in two different proportions (7:2 and 9:1).

Lasic, described that cycles of freeze and thaw increased the encapsulation efficiency to values up to 50%. [141] Similarly, in this work, the influence of cycles of freezing and thawing was evaluated.

Finally, the influence of extrusion and extrusion temperature in the EE was evaluated also and taken in account in the optimization process. Figure 15 summarizes the optimization process.

In the end, after the optimization process, the final formulations used in this work were DPPE:CHEMS 7:3 and DPPE:CHEMS:SA 7:2.5:0.5 in the MLV (MLV 7:3 and MLV SA, respectively) and in LUV (LUV 7:3 and LUV SA, respectively) structure containing 1 mg/mL of indomethacin, 5 mM of lipid and after 10 freeze and thaw cycles.

The parameters used to assess the best liposomal formulation were size, potential zeta and encapsulation efficiency for all the formulations obtained.

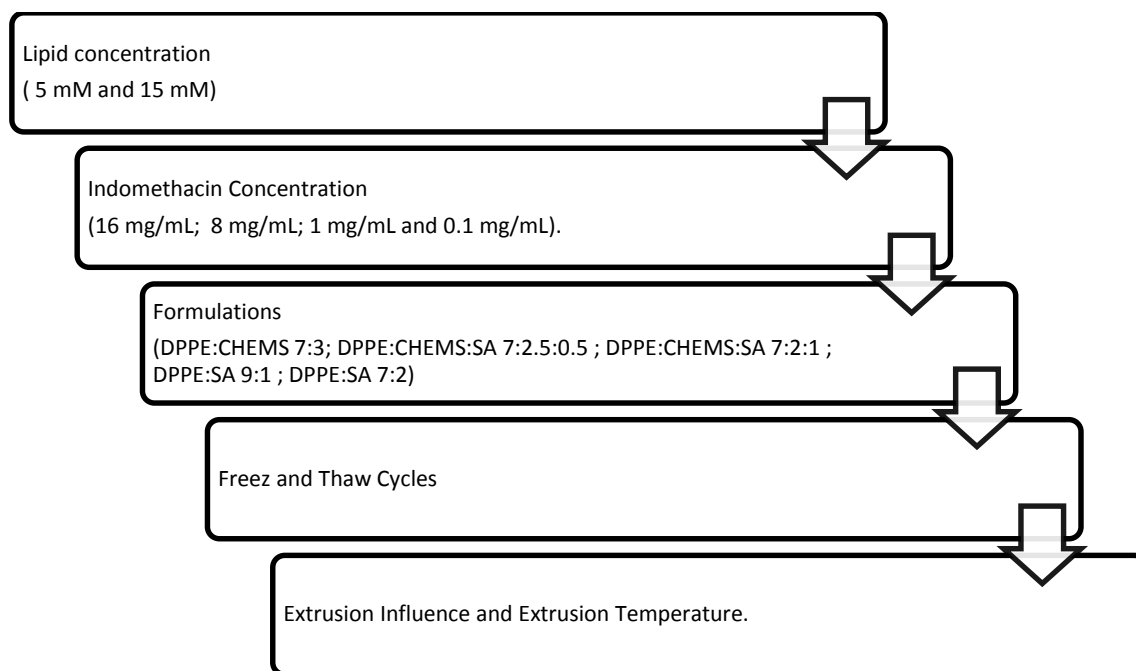


Figure 15 - Parameters used for Liposomal production optimization.

1.2.1 Lipid Concentration

The first step towards optimization, was the use of different lipid concentrations and its effect on EE, size and zeta potential. The desired amount of lipids was added as well as the amount of indomethacin and the liposomes were produced. For the formulation containing 5 μM of lipids, 12.10 mg of DPPE and 3.65 mg of CHEMS were weighted, whereas for the formulation containing 15 μM of lipids, 36.30 mg of DPPE and 10.95 mg of CHEMS were weighted. The procedure was then followed as explained previously.

At this point, formulation containing SA had not yet been introduced.

1.2.2 Indomethacin Concentration

Secondly, the influence of indomethacin concentration was assessed. In order to reach the indomethacin concentration that was more suitable for this specific formulation, several concentrations were tested (16 mg/mL; 8 mg/mL; 1 mg/mL and 0.1 mg/mL). The desired amount of indomethacin was weighted, dissolved in a solution of 3:1 methanol/chloroform and added to the organic phase.

1.2.3 Formulations

Even though several formulations were produced until this step, the encapsulation efficiency remained at very low values. SA was inserted in this step. In order to prepare these new liposomes four different formulations were produced: (DPPE:CHEMS:SA 7:2.5:0.5; DPPE:CHEMS:SA 7:2:1 ; DPPE:SA 9:1 ; DPPE:SA 7:2). These liposomal formulations add a final

lipid concentration of 5 mM and a concentration of indomethacin of 0.1 mg/mL. The lipids and indomethacin were weighted, dissolved in a solution of 3:1 methanol/chloroform and placed in the rotary-evaporator. The protocol was followed as previously described.

1.2.4 Cycles of Freeze and Thaw

In order to improve encapsulation efficiency cycles of freeze and thaw were performed. In this assay, after lipidic film formation and vortexing, the liposomal suspension was transferred to an eppendorf (1.5 mL in each eppendorf) and the eppendorfs placed freezer at -80°C for 6 minutes. After this period, the eppendorfs were transferred to a water bath, at 60 °C, for 4 minutes.

1.2.5 Extrusion Influence

The effect of extrusion on encapsulation efficiency was another factor evaluated in this work. The liposomal suspensions were produced as previously described and half was extruded while the other half was the final product of MLV. The encapsulation efficiency, size and potential zeta of the non-extruded and extruded liposomes, MLVs and LUVs respectively was measured and used as a comparison measurement.

Also, extrusion temperature was changed. Initially, extrusion temperature was set to 42°C, however, to achieve a temperature near the transition temperature, it was raised to 65°C.

1.3 Liposomes Characterization

1.3.1 Characterization of liposomes size and Zeta Potential

To determine Particle Size and Zeta Potential, the liposomal formulations were diluted 1:10 in HEPES Buffer and 2 mL were placed inside a cuvette for the measurement. Both size and zeta potential measurements were performed in a Brookhaven BI-MAS and Zeta-PALS (Brookhaven Instruments, Holtsville, NY, USA). For each formulation 6 measurements were made and three independent measurements were carried out to achieve statistical significance.

1.3.2 Phase transition temperature

The phase transition temperature of liposomes was determined to assess if (a) the addition of SA in the liposomes affected their physical properties, and (b) indomethacin encapsulation affected liposomes structure. To perform this task, size was measured through a temperature range (37-74) °C in Zeta Pals. The count rate was analyzed for each temperature and a graphical representation of count rate versus temperature performed. T_m and cooperativity were determined using Origin©.

1.3.3 Morphology

Morphological evaluation was carried out on TEM. Since the main objective was to evaluate morphological changes between the formulations and at different pHs, the liposomes were prepared and morphology evaluated at pH 7.4 and at pH 5. For morphology analysis at pH 7.4 samples were diluted 1:5 in HEPES buffer. For analysis at pH 5, liposomal formulation at pH 7.4 was diluted 1:5, centrifuged 30 minutes at 2000 rpm, 25°C. The supernatant was removed and the liposomes resuspended in Acetate buffer, pH 5.

Samples were deposited on support grids made of Cu that possess an ultramicrotomy mesh. Their dimensions were of 3 mm of diameter, 100 µm of edge thickness, and they are electron transparent in the mesh region. Uranyl acetate was used as a negative staining for samples of biological origin. Since it deposits uranium atoms in specific regions of the specimen, that way absorbing electrons from the beam, it enhances the contrast, facilitating the imaging.

A fluorescent screen is responsible for TEM imaging, which can also be coupled to a photographic film, or an image recording system. Projector lenses expand the electron beam onto the imaging device.

The morphology of the liposomes was determined by TEM (Jeol JEM-1400, Tokyo, Japan). About 10 µL of the aqueous dispersion of liposomes was placed on copper grids and after 1 minute excess was removed and the sample stained with an aqueous solution of 1% uranyl acetate for 30 seconds. Samples were then observed in a microscope at the accelerating voltage of 60 kV.

1.4 Encapsulation Efficiency and Loading capacity.

Encapsulation Efficiency was assessed using a UV/VIS spectrometer. The EE measures liposomes ability to encapsulate drugs based on the amount of drug placed during the production and the amount of drug in the liposome, equation 2. Also, loading capacity was evaluated. The LC correlates the amount of lipid and the amount of drug, equation 3.

Firstly there was the need to produce a calibration line for indomethacin. To perform this task, 0.7 mg of indomethacin were weighted and added to 25 mL of HEPES Buffer, which produced an indomethacin solution with a concentration of 78.26 µM. Dilutions were made to achieve concentrations of between a range of 5 to 60 µM. The absorbance was measured in a PerkinElmer Lambda45 UV/Vis spectrometer, in the range 200-600 nm. The indomethacin peaks were found at 320 nm and 266 nm, which is in concordance with other authors [142] and based on the values it was obtained a two calibration curves, Figure 16.

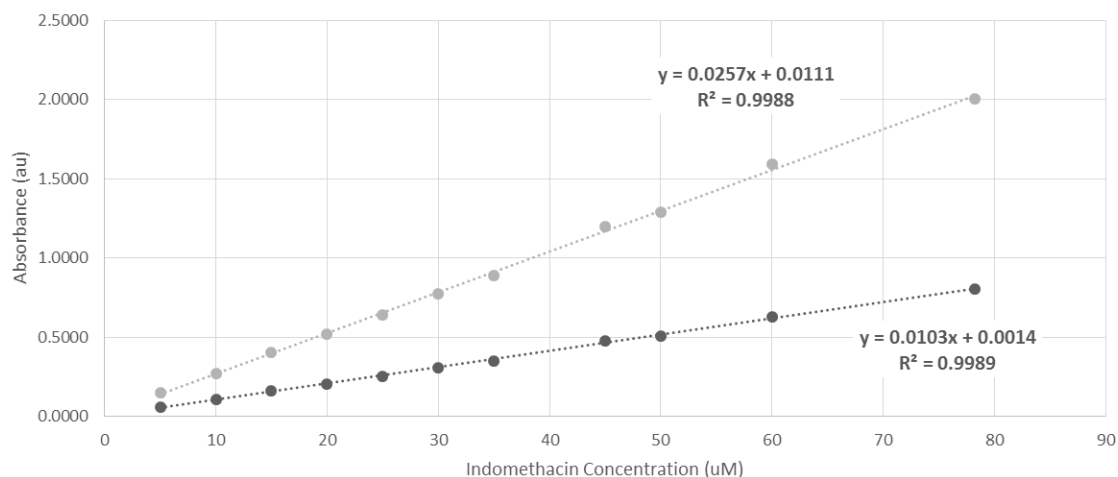


Figure 16- Indomethacin calibration curves for PerkinElmer Lambda45 UV/Vis spectrometer.

To assess EE and LC the amount of indomethacin that was not entrapped in the liposomes (free indomethacin) was determined. To do so, 100 μ L of liposomes suspension was along with 1.4 mL of HEPES buffer were placed inside centrifugal filter units, Amicon Ultra-4, PLGC Ultracel-PL membrane, 10 kDa, Milipore) and centrifuged at 1000 rpm, 25°C, for 28 minutes. The supernatant was then analyzed in the UV/Vis spectrometer and the amount of indomethacin determined using the calibration line.

The amount of drug in the liposome was calculated subtracting the amount of free indomethacin to the total amount of indomethacin. EE and LC were then calculated from the above equations.

1.5 Drug Release

The ability to release indomethacin at pH 5.0 and at pH 7.4 was also evaluated. To do so, 1.5 mL of liposomal suspension were placed into a dialysis bag of cellulose with molecular weight cut off of 3500 Da, Cellu Sep, Membrane Filtration Products, Inc. The dialysis bags were placed in 40 mL of buffer, Acetate or HEPES and the media stirred with a magnetic bar at 300 rpm at 37°C. At time points 15 min, 30 min, 60 min, 90 min, 120 min, 180 min, 240 min 12 hours and 24 hours, and 48 hours, 300 μ L of the suspension were removed placed on a 96 well-plate and read in a plate reader, Synergy HT, BioTek [®] Instruments, Inc., in the range 200-400 nm.

A new calibration line was performed for this equipment and the amount of indomethacin present in the medium calculated based on it. The amount of indomethacin released from the liposomes was then calculated based on Equation 4.

1.6 Stability Assays

Drug stability is one of the parameters that have to be taken in account when producing a new drug. In order to assess formulations stability size and potential zeta of each formulation (MLV 7:3, MLV SA, LUV 7:3 and LUV SA) were evaluated for one month. To perform this task, the liposomal suspension was diluted 1:10 in HEPES buffer and the suspension stocked in the fridge at 4°C, protected from light. For each measurement, 2 mL of suspension were removed, placed inside a cuvette in the DLS. After the measurement the suspension was stocked again. Placebo solutions were also tested in terms of stability to infer if indomethacin affected the liposomes stability. Two independent assays were performed. These measurement were carried out in Zeta Pals as previously explained.

1.7 *In vitro* Assays

Cells response to liposomes was evaluated using a several tests such as cytotoxicity evaluation and uptake assays.

1.7.1 *Cell Culture*

Both Raw and L929 were cultured in Dulbecco's Modified Eagle Medium, DMEM, from Invitrogen. The medium was supplemented with 10% Fetal Bovine Serum, FBS, from Gibco, 1% Penicillin Streptomycin, Pen Strep, Invitrogen and 1% Fungizone, Invitrogen. Cells were allowed to grow at 37°C, 5% CO₂ and 95% humidity. Before reaching confluence cells were passed. Raw cells were washed with Hank's Balanced Salt Solution, HBSS, from Invitrogen, and detached using a scrapper and resuspended in fresh DMEM. Subculture was done at a proportion 1:6. Subculturing of L929 cells involved a more complex procedure using trypsin, Invitrogen, to detach cells. Cells were washed with HBSS, 2mL of trypsin added and incubated for 10 min. After this period, 4 mL of fresh DMEM were added and the cells centrifuged at 1500 rpm, 25°C for 10 minutes. The supernatant was removed and 5 mL of fresh medium were added. Subculture was done at a proportion 1:4.

1.7.2 *Cell Viability*

As said in the previous chapter, cell viability was assessed by the colorimetric method MTT assay. Cells were detached using the procedure described before and counted in a Neubauer chamber. After counting cells were seeded at a density of 5 000 cells/well for Raw 264.7 and 50 000 cells/well for L929 in a 96 well plate.

Meanwhile, the liposomal formulations were diluted in complete DMEM to achieve concentration of 5 µM, 10 µM, 25 µM, 50 µM and 100 µM of indomethacin. Placebo formulations of all the suspensions were also prepared using the same amount of liposomes. As the main

objective of this assay was to evaluate drug cytotoxicity, there was the need to run controls. The positive control used to this assay was cells incubated with fresh DMEM and the negative control only DMEM. To evaluate the effect of the drug and to compare it with the liposomal formulations indomethacin at the same concentration as in the liposomes was also incubated. In the end, for each concentration evaluated the conditions were negative control, positive control, indomethacin, MLV 7:3 placebo, MLV 7:3, MLV SA placebo, MLV SA, LUV 7:3 placebo, LUV 7:3, LUV SA placebo and LUV SA.

Cells were allowed to grow for 24 hours, the medium was removed and 200 μL of medium or medium containing liposomes were added to each well. The plates were then incubated for 24 hours. After the incubation period, the well were washed with HBSS, 180 μL of fresh DMEM were added to each well along with 20 μL of MTT, Sigma, at 5 mg/mL In HBSS.

After this period, the medium was removed and 200 μL of Dimethyl Sulfoxide (DMSO), Sigma, were added to each well and allowed to dissolve for 30 minutes. Absorbance was read in a plate reader, at 590 nm with reference to 630 nm.

The percentage of viability was calculated comparing the absorbance in the well with the positive control after subtraction of negative control. After, IC50 was calculated using GraphPad Prism®, GraphPad Software, Inc. A non-linear regression was performed and the equation that correlates the concentration logarithm with the response was used. IC50 was then calculated by interpolation. Two independent assays containing five replicas each were carried out.

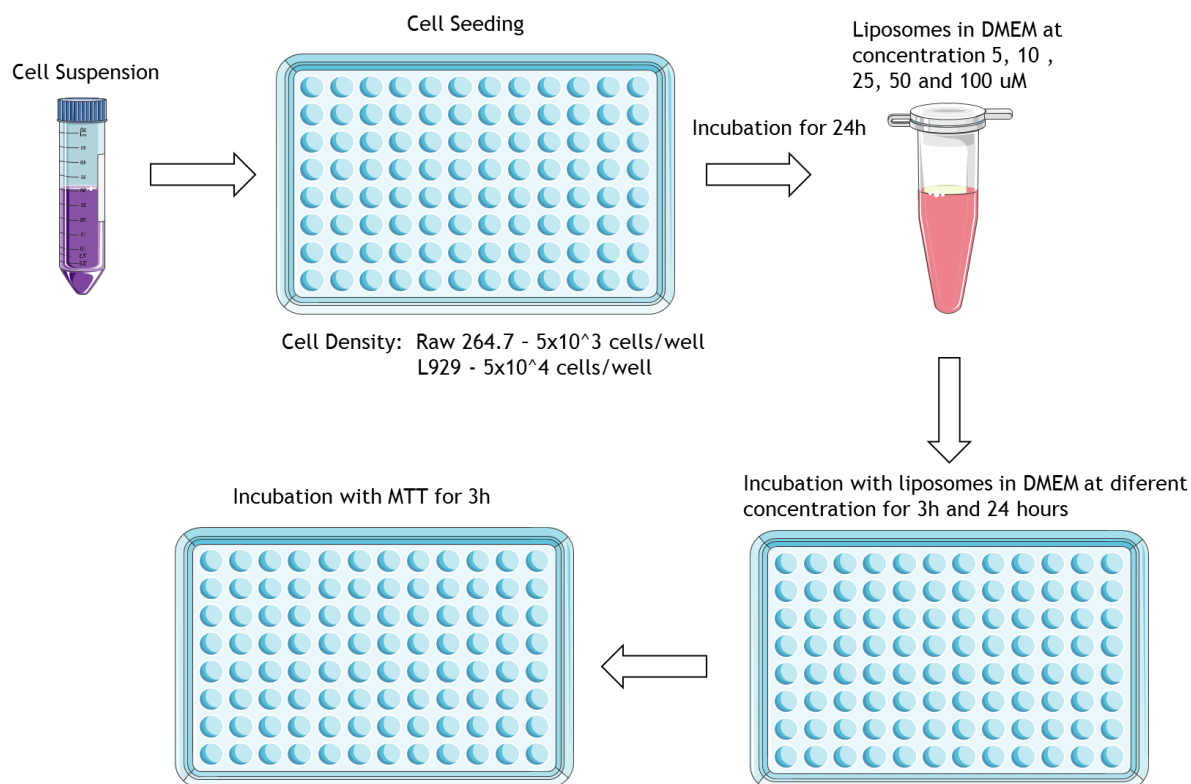


Figure 17 - Schematic representation of the viability assay, adapted from[123].

1.7.3 Uptake

Liposomes with fluorescent characteristics were produced by the addition of 1,2-dipalmitoyl-sn-glycero-3-phosphoethanolamine-N-(7-nitro-2-1,3-benzoxadiazol-4-yl), NBD, from Avanti Polar Lipids, which possesses fluorescent characteristics. NBD was added at 1 mol % of the amount of lipid and added to the organic phase. Liposomes were produced as previously described.

Round cover glasses were sterilized and placed in a 24 well plate. 27 780 cells/well were seeded and allowed to grow for 24 hours. Meanwhile, liposomes dilutions in DMEM were done to achieve indomethacin concentrations of 5, 25 and 100 μM . After the incubation period, 400 μL of the diluted liposomal formulations were added and incubated for 3 hours. DMEM was removed and the wells rinsed 3 times with HBSS. Cells were fixed for 30 minutes in 2% paraformaldehyde, in DMEM (v/v) and rinsed thrice with HBSS. After, they were permeabilized with 0.2% (v/v) Triton x-100, Sigma, in HBSS, under stirring for 10 minutes. Triton was removed and the wells washed 3 times with HBSS. The samples were then incubated in DAPI diluted 1:10 000 in HBSS for 10 minutes at resting temperature under stirring. After, samples were rinsed thrice with HBSS, the cover slips removed from the wells, one drop of Vectashield, Vector Laboratories, was add to each sample and placed on a microscope slide. Samples were then visualized under a Nikon Eclipse E400 fluorescence microscope.

1.8 *In Vitro* permeation

Samples or porcine skin ear were excised, dissected and the skin surface was cleaned to remove hairs and subcutaneous fatty tissue. The skin was then cut into pieces of approximately 1 cm^2 and placed in the Franz diffusion cells, PermeGear, Hellertown, USA. The exposed surface was 0.64 cm^2 . 5 mL of Hepes buffer containing 5% ethanol (v/v) were placed in the receptor side of the diffusion cell. Also, a magnetic stir bar was placed in this compartment. 600 μL of liposomal formulations was placed in the donor side of the Franz cell and covered with parafilm. A negative control, composed of Hepes Buffer was used as a baseline control in order to remove the interferences of porcine skin. At time points 0, 1h, 2h 3h 4h, 5h, 6h, 7h and 8h, 300 μL were taken and placed in a 96 well plate. The same volume was replaced into the diffusion cell, and bubbles formed below the skin removed. The absorbance was measure in the range 200-400 nm in a plate reader. Two independent assays were performed.

1.9 Statistical Analysis

Statistical analysis was performed using SPSS®, IBM. For all the experiments the results are expressed as mean \pm standard deviation. One-way Anova was performed using Tuckey's and Dunnet post-hoc test. Dunnet's post-hoc test was done when there was the need to compare different groups with a control. A p-value of 0.05 was considered as statistical significant.

Chapter 6 - Results and Discussion

1. Optimization of liposomes production

The first step to achieve a formulation with the desired characteristic was the optimization. The main factor taken into account was the EE of the formulations. Several procedures were performed to measure the EE, since the initial procedure was not suitable once it promoted indomethacin release from the liposomes.

Initially, liposomes containing 0.1 mg/mL of indomethacin with and without SA and in the MLV and LUV structure were made. However, after the achievement of a suitable method to measure the EE it was found that the liposomes were capable of incorporating a higher amount of indomethacin. Due to this, the amount of indomethacin was increased to a concentration of 1 mg/mL.

The number of freeze and thaw cycles was evaluated in a range from 0 to 10 cycles. After the analysis it was found that 10 was the amount of cycles which produced the highest EE, and this number set to be the cycles used from this point.

Finally, after this process, four different formulations were produced and characterized: DPPE:CHEMS 7:3 and DPPE:CHEMS:SA 7:2.5:0.5 in the MLV (MLV 7:3 and MLV SA, respectively) and in LUV (LUV 7:3 and LUV SA, respectively) structure containing 1 mg/mL of indomethacin, 5 mM of lipid, after 10 freeze and thaw cycles.

2. Liposomes Characterization

As said previously liposomes were characterized in terms of size, zeta potential, EE and LC and morphology. The following section presents the results obtained.

2.1 Size

In table 8 it is possible to observe the data obtained for liposomes size and polydispersity. It is possible to observe that MLV SA are the larger with mean size of 436 nm whereas LUV SA placebo are the smaller liposomes 75 nm. There seems to be no statistical significant difference between placebo and indomethacin containing liposomes for all the formulations evaluated. Also, differences between MLVs and LUVs of the same formulation were tested and it only seems to appear statistical significant differences between MLV SA and LUV SA.

Table 8 - Liposomes size and polydispersity. Mean and standard deviation of three independent samples. (*) Statistical significant differences, $p < 0.05$.

		Size (nm)	Polydispersity
MLV 7:3	Placebo	222 ± 121	0.27 ± 0.04
	Indo	197 ± 70	0.36 ± 0.02
MLV SA	Placebo	259 ± 84	0.26 ± 0.06
	Indo	436 ± 90 *	0.34 ± 0.06
LUV 7:3	Placebo	111 ± 19	0.037 ± 0.009
	Indo	103 ± 82	0.122 ± 0.002
LUV SA	Placebo	75 ± 6	0.13 ± 0.03
	Indo	121 ± 27 *	0.081 ± 0.001

Polydispersity is a measure of heterogeneity of a suspension. If particles are monodisperse, which means, they have the same size while on a polydisperse formulation more than one population may exist. A formulation is considered monodisperse if the value of polydispersity is below 0.2. It is possible to observe that LUV have smaller values of polydispersity than MLV. This result was expected since the extrusion process allows the formation of liposomes with controlled size.

The fact that size is much higher in the SA formulations (although is not statically different) when indomethacin is present comparing with the placebo, has do to with the fact that indomethacin establishes electrostatic bonds with the SA molecules, increasing thereby the space occupied in the solvation layer. This occurrence is even more pronounced in the case of the MLVs, once they present more than one bilayer which enhances the phenomenon, conferring a higher increase in the liposome dimensions. In the case of the formulations that do not contain SA, the size slightly decreases when indomethacin is present which is probably due a closer packing of the lipids molecules.

2.2 Zeta Potential

Table 9 presents the results obtained for the liposomes Zeta Potential. MLV 7:3 present the higher zeta potential while LUV SA present the lower values. No statistical significant differences were found between each formulation. The addition of indomethacin induced an

increase in zeta potential in the MLVs, which was not statistical significant, however this did not occur in LUVs.

A value zeta potential below -30 mV is desirable since at this value of zeta potential occurs repulsion between liposomes instead of aggregation. It is possible to notice that all the formulations have zeta potential values around the -30 mV whereby it is possible to say that this formulations are stable in terms of zeta potential.

Table 9 - Zeta Potential of the liposomal formulations (mean and standard deviation of three independent samples).

		Potential Zeta (mV)
MLV 7:3	Placebo	-50 ± 9
	Indo	-36 ± 5
MLV SA	Placebo	-42 ± 13
	Indo	-34 ± 4
LUV 7:3	Placebo	-28 ± 6
	Indo	-28 ± 2
LUV SA	Placebo	-28 ± 2
	Indo	-25 ± 3

2.3 Encapsulation Efficiency and Loading Capacity

In table 10, the results of EE and LC are presented. EE, as said previously is correlated with the ability to entrap indomethacin in the liposomes while LC is a measure of comparison between amount of indomethacin and the amount of lipid. MLV SA are the ones who had the ability to entrap the higher amount of indomethacin. However, there is no statistical significant differences between the EE and the different liposomal formulations.

Table 10 - Entrapment Efficiency and Loading Capacity. Mean ± Standard deviation of three independent samples.

Encapsulation Efficiency				Loading Capacity		
MLV 7:3	60%	±	3%	18,8%	±	0.8%
MLV SA	69%	±	5%	22%	±	2%
LUV 7:3	61%	±	8%	18%	±	1%
LUV SA	63%	±	10%	20%	±	3%

In which concerns LC for all the formulations evaluated was around the 20% for all the formulations evaluated. MLV SA were the liposomes that possess the highest value of LC

whereas LUV 7:3 were the ones with the lowest values. The LC differences among all the formulations tested is not statistically significant. The addition of SA enhanced the EE, possibly due to electrostatic bonds between SA and indomethacin, but not as much as could be expected.

2.4 Morphology

Morphology was assessed using TEM and representative images of each type of liposomes can be visualized on figure 19. In figure 19 A and B it is possible to observe MLVs 7:3 and MLVs SA, respectively, in Hepes buffer, pH 7.4. These formulations present liposomes with round shape morphology containing populations of liposomes with different sizes.

Figure 19 C and D is representative of MLVs SA placebo and MLVs SA, respectively, in acetate buffer, pH 5. It is possible to observe that for both formulations that was a complete loss of structure when compared to MLVs SA at pH 7.4. The round shape morphology of liposomes was destroyed. This morphology can be explained with hexagonal phase formation. DPPE is a phospholipid that presents conic geometry due to presence of a less bulky polar group when compared to its hydrocarbon chains. When there is no stabilizer, at neutral pH it forms a hexagonal phase (Figure 18). The addition of CHEMS helps in the formation of a stable lipid bilayer due to repulsion of the phosphate groups of the phospholipid with the carboxylate groups of CHEMS. At neutral pH, CHEMS is deprotonated, however, when the pH lowers, it occurs protonation of carboxylate groups and the repulsion with phosphates stops, leading to bilayer destabilization. [124]

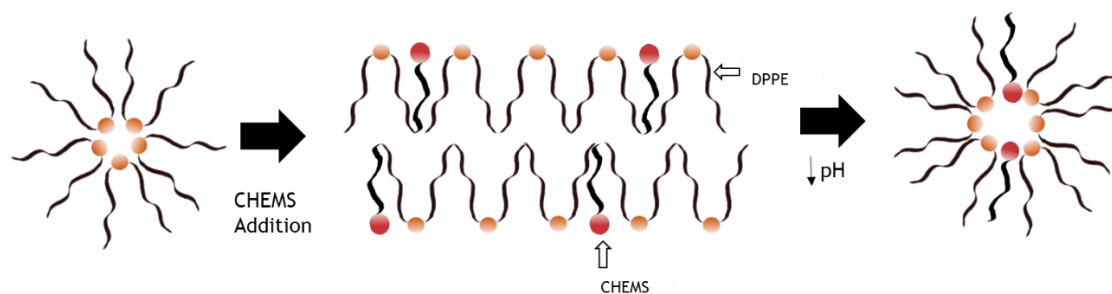


Figure 18 - Destabilization of lipid bilayer and hexagonal phase formation.

Figure 19 E and F presents TEM representative images of LUV 7:3 placebo at pH 7.4 and 5, respectively. It is possible to notice that LUV 7:3 placebo at pH 7.4 present a round shape morphology with populations much more uniform than MLV 7:3. At pH 5, the liposomes do not lose the round shape however they became very small when compared with the ones at pH 7.4 and with several populations.

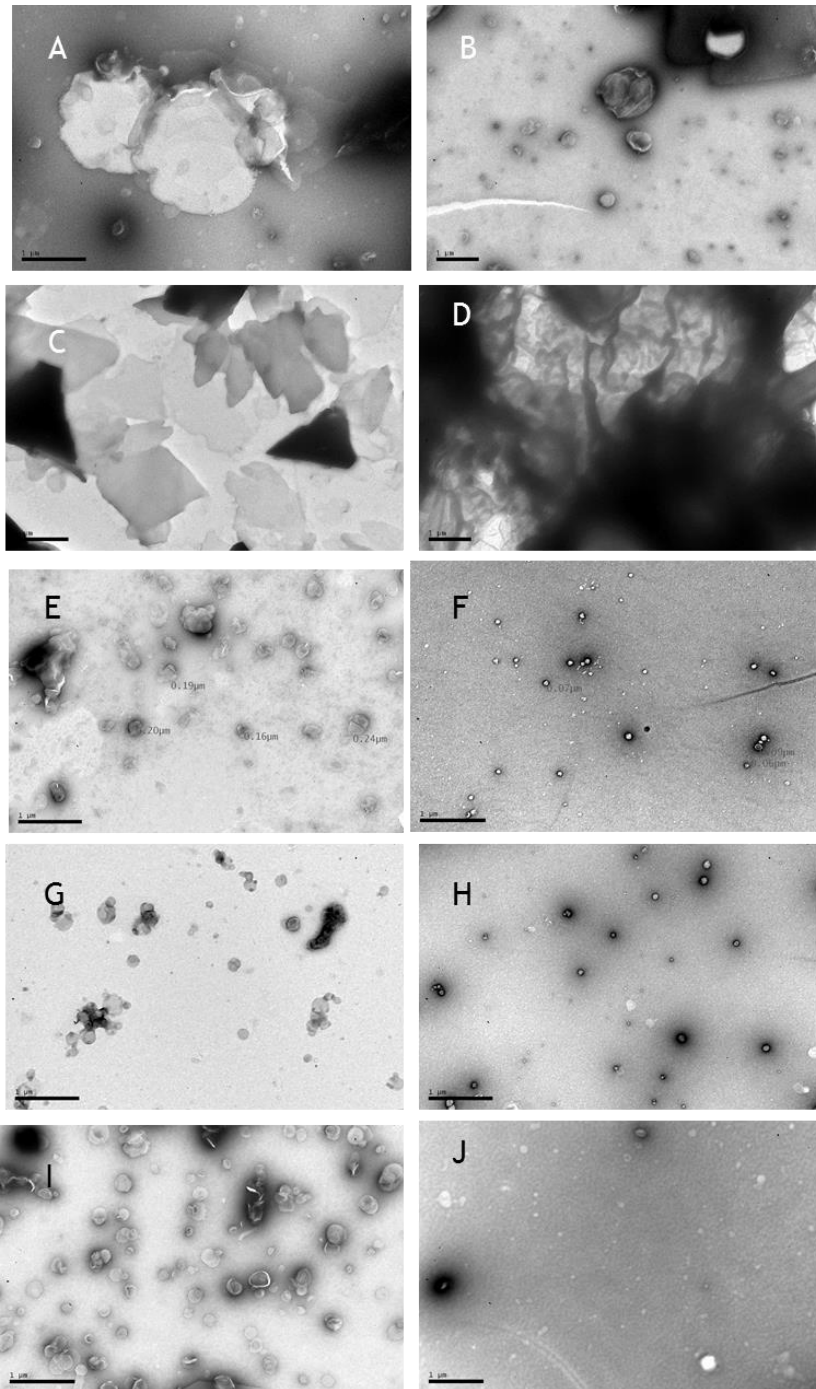


Figure 19 - TEM representative images of liposomes, (scale bar = 1 μm). (A) MLVs 7:3 in Hepes Buffer; (B) MLVs SA in Hepes Buffer; (C) MLVs SA placebo in Acetate Buffer; (D) MLVs SA in acetate buffer; (E) LUVs 7:3 placebo in Hepes buffer; (F) LUVs 7:3 placebo in Acetate buffer; (G) LUVs 7:3 in Hepes buffer; (H) LUVs 7:3 in Acetate buffer; (I) LUVs SA in Hepes buffer and (J) LUVs SA in Acetate buffer.

LUV 7:3 at pH 7.4 and pH 5 are presented in figure 19 G and H. It is possible to notice that the above mentioned behavior for placebo formulations occurs also to the formulations containing indomethacin. In this case, it is possible to notice that indomethacin did not have the stabilization effect that had in the MLV.

Last but not least, figure 19 I and J present TEM images of LUV SA in Hepes buffer and Acetate Buffer, respectively. At pH 7.4, the liposomes are in a round shape morphology with uniform sizes. However, at pH 5, the liposomes are have only a few nanometers which may indicate that they have formed micelles instead of a lipid bilayer. Also, in this case, the addition of indomethacin seems to not have a stabilizing effect at low values pH.

2.5 Stability

Liposomes stability was evaluated throughout a month and Figure 20 is representative of the results obtained for size and zeta potential measurements. It is possible to notice that LUVs are more stable than MLV. LUV 7:3 is the formulation which is more stable throughout the evaluated period since they suffer smaller changes in effective diameter than all the other formulations tested.

Lasic described that freeze and thaw cycles promoted liposomes aggregation and this behavior can be found mainly in MLV [141]. LUVs also undergo freeze and thaw cycles, however the extrusion is only done after the cycles which may promote their stabilization. While after the first measurement, LUVs increase in size and then had the tendency to stabilize, MLV did not show any tendency to stabilize showing size fluctuations for each time point.

Zeta potential variations occurred both for MLV and LUV and it appear that the same behavior can be found for all the formulations. Initially, zeta potential seems to decrease and at a time point between 11-14 days it seems to increase.

In conclusion, in which concerns stability, it is possible to say that LUVs seems to be more stable than MLV regarding size. On the other hand, regarding zeta potential, all the liposomal formulations do not seem to be stable. Nevertheless, the zeta potential was always above -25 mV, which justifies the fact that the size did not change so much, once they still had sufficient surface charge to repel themselves and do not aggregate. To increase stability throughout time, liposomes could be freeze-dried however the optimizations of this procedure is time-consuming and due to lack of time the possibility to study this method was not possible.

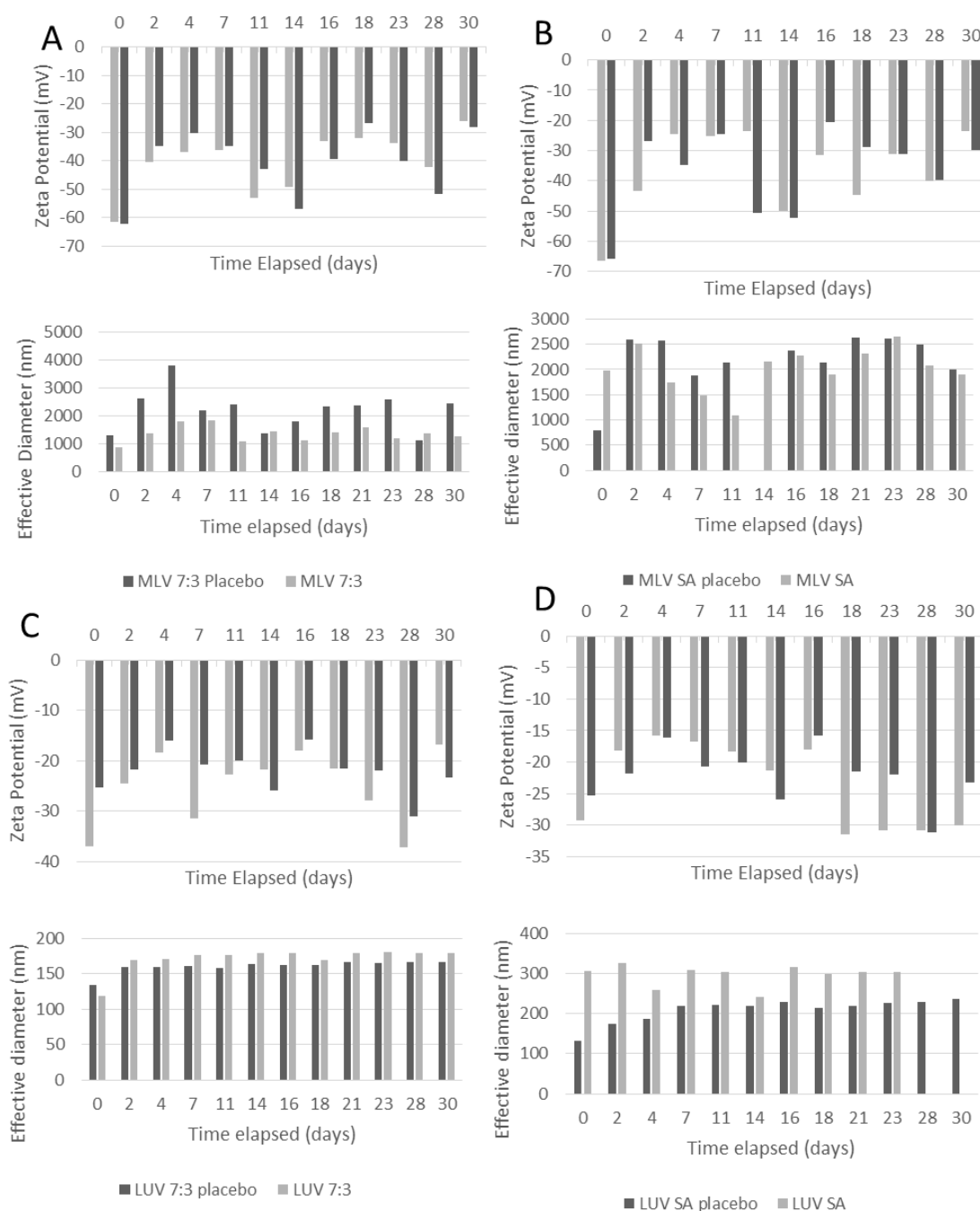


Figure 20 - Liposomes Stability evaluated through a month. Zeta Potential and Size measurements are presented. A - MLV 7:3; B- MLV SA; C - LUV 7:3; - D- LUV SA.

2.6 Phase Transition

In Table 11 and Figure 21, the results from phase transition are presented. It is possible to observe that the higher T_m was found for MLV SA, 62.9 °C, whereas the highest value of cooperativity was found for MLV 7:3, 3389. DPPE for itself has a phase transition temperature of 63°C, according to Avanti Polar Lipids, and Handa et. al reported that DPPE had a phase transition of 64.5 °C [141]. Ohtake et al. [142] found that cholesterol addition to liposomes had

a fluidizing effect in the membrane. It was possible to observe that for all the formulations evaluated the values were below the 63°C registered for DPPE, which is possibly related to the addition of CHEMS, a derivative from cholesterol. Regarding indomethacin addition to liposomes and its effects on T_m it was found that indomethacin promoted the decrease of phase transition temperature. This effect plus the fact that the cooperativity almost is unperturbed is most possibly due to its interaction with the polar headgroups of the phospholipids.

Table 11 - Phase transition temperature and cooperativity values of MLV SA placebo, MLV 7:3 and MLV SA formulations.

	MLV SA placebo	MLV SA	MLV 7:3
T_m (°C)	62.9 ± 0.3	59.8 ± 0.4	62.2 ± 0.2
Cooperativity	1364 ± 203	1297 ± 222	3389 ± 104

The MLV 7:3 present a much higher cooperativity than the MLV SA, which is related to the fact that in the second case we have the addition of one more molecule in the bilayer, making it more heterogeneous and more fluid which also justifies the lower T_m .

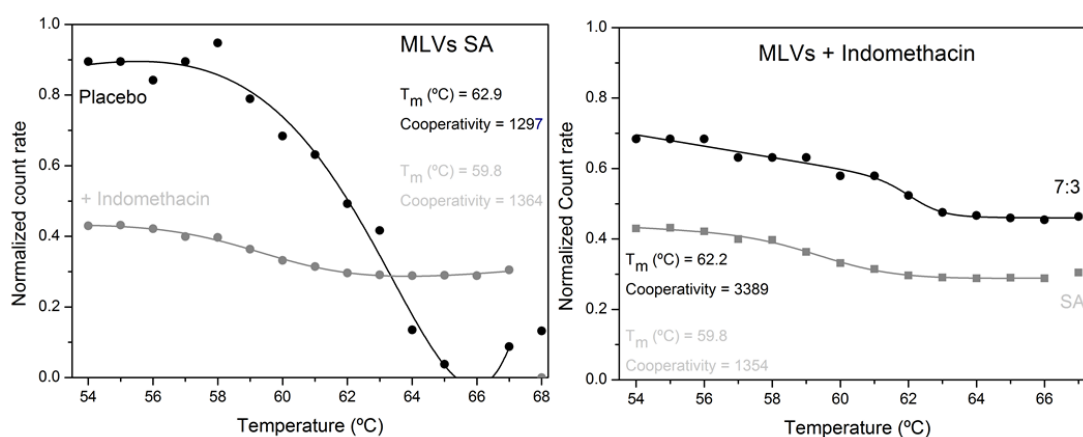


Figure 21 - Normalized count rate vs temperature.

3. Release assay

In vitro release studies were performed to estimate the release patterns of the formulation over a period of 32 hours. Figure 22 summarizes the release profiles for all the formulation evaluated. From this figure it is possible to understand two different behaviors (a) the behavior of liposomes at pH 7.4 and (b) and the behavior at pH 5. Against what was expected, indomethacin release was found to be higher at pH 7.4 than at pH 5. Furthermore, liposomes at pH 7.4 steady the amount of indomethacin released after 5 hours while at pH 5 it only took 3 hours to achieve this equilibrium.

At pH 7.4, the highest release was found for LUV SA whilst the lower release was found for MLV 7:3. Also, for all the formulations containing SA it was found that they had the highest release rates (0.6 %). Although, at both pHs, the release rates were very small which means that the drug is almost not released from the liposomes, which is a desirable characteristic at pH 7.4.

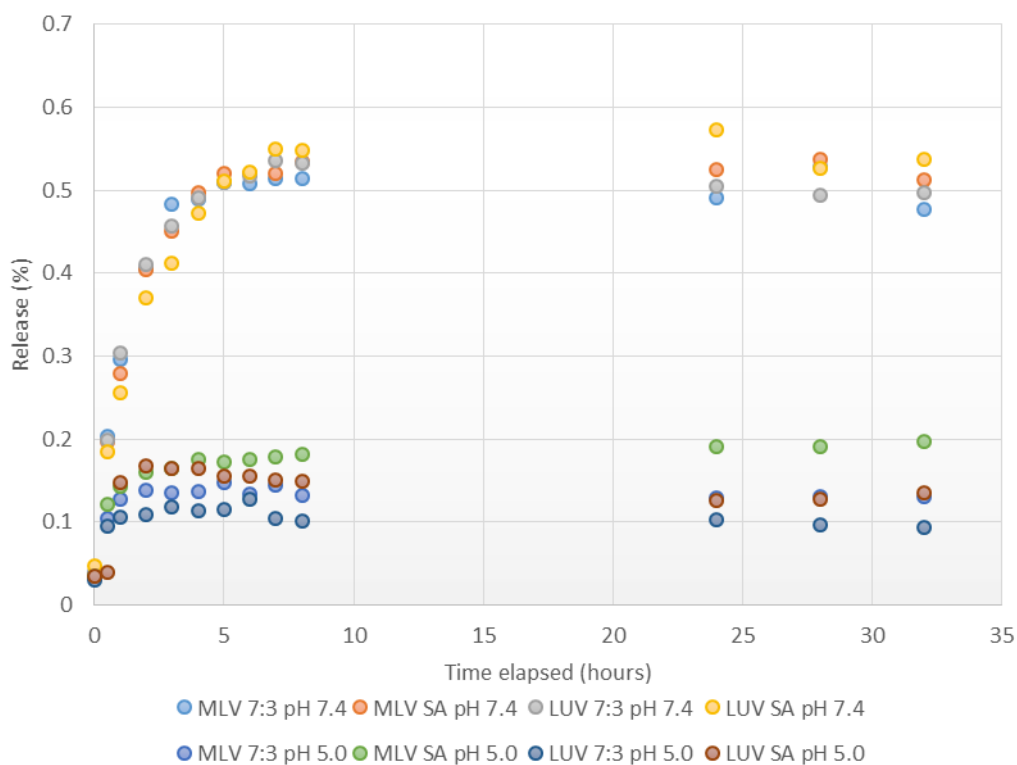


Figure 22 - *In vitro* release profiles for MLV 7:3, MLV SA, LUV 7:3 and LUV SA.

Taking in account the results from TEM, in which indomethacin lead to a bilayer stabilization, it is possible that the low values of release at pH 5 may happen due to interactions with the lipid bilayer. Although these results were not expected they might be positive. If the drug is not released at pH 5, when crossing the skin, which possesses a region with pH around 5, the drug is not released thus not delivering drug to a non-inflamed site.

Thereby if the formulations reach their target, there they will be disintegrated, converted into lysolipids and fatty acids, resulting for sure in the release of the encapsulated drugs specifically at the diseased target site.

4. *In vitro* studies

4.1 Cytotoxicity

The IC₅₀ was calculated after 24 hours of incubation with the liposomes and the results are presented in table 12. During the cytotoxicity studies, a concentration range of 5-100 μM of indomethacin was used, however, as shown in table 12 it was not possible to find the IC₅₀ for indomethacin and several placebo formulations (N.D.). For some cases, although they are out of range, it was possible to extrapolate the IC₅₀ values using the aforementioned software. Also, for the fibroblast cell line, it was not possible to calculate the IC₅₀ but for MLV 7:3. In order to overcome this issue, additional studies may be performed using a wider concentration range, for example 1 - 1000 μM of indomethacin.

Table 12 - IC₅₀ values of indomethacin and liposomal formulation for Raw 264.7 and L929.

	Raw 264.7	L929
Indomethacin	N.D. ²	N.D.
MLV 7:3 placebo	N.D.	N.D.
MLV 7:3	51.29 μM	184.93 μM
MLV SA placebo	224.39 μM	N.D.
MLV SA	66.83 μM	N.D.
LUV 7:3 placebo	254.68 μM	N.D.
LUV 7:3	73.45 μM	N.D.
LUV SA placebo	N.D.	N.D.
LUV SA	87.9 μM	N.D.

For all the cell lines and concentration evaluated, indomethacin did not present an IC₅₀ which is in concordance with previous studies. For the fibroblast cell line studied, it was only possible to define an IC₅₀ value for MLV 7:3, 184.93 μM while for all the other formulations these values were not defined. This means that, in the concentration range evaluated, only MLV 7:3 present some toxic effects.

On the other hand, for Raw 264.7 macrophage cell line, all the formulations containing indomethacin presented an IC₅₀ value in the range studied. However, for some placebo formulations, such as MLV 7:3 and LUV SA, it was not possible to determine the IC₅₀ value.

² N.D. - not defined

Based on the analysis performed until this moment, it is possible to conclude that all the formulations evaluated had a more marked effect on macrophage than on fibroblasts. This effect may happen due to the macrophage ability to internalize invader particles. Macrophages have the ability to internalize vesicles from 50 -300 nm by clathrin-mediated endocytosis, phagocytosis, macropinocytosis, caveolae-mediated endocytosis and non-clathrin-non-caveolae-dependent endocytosis. [143] However, fibroblasts do not have internalization mechanisms as developed as macrophage which may explain the results obtained for IC50 determination.

4.2 Uptake

Uptake was assessed by fluorescence microscopy after 3 hours of incubation with macrophages and the pictures are presented in figure 23. Figure 23 A presents the control and figure 23 B and C presents the MLV 7:3 at a concentration of 100 μ M. For all the other formulations tested it was not possible to find any traces of liposomes.

Looking at Figure 23, it is possible to notice a change in macrophage conformation after the addition of liposomes. In the control, the macrophage are in an activated state, which is confirmed by their spread morphology. However, when in contact with liposomes, they present a round-shape morphology which seems to indicate an inactivated state. In order to assess if the macrophage are in a pro-inflammatory state or not, several assays should be performed to determine the presence of TNF α and/or cytokines.

Regarding, liposomes interaction with the macrophage, apart from the change in morphology suffered by the macrophage, it is possible to notice that the liposomes did not had the time to penetrate in the nuclei.

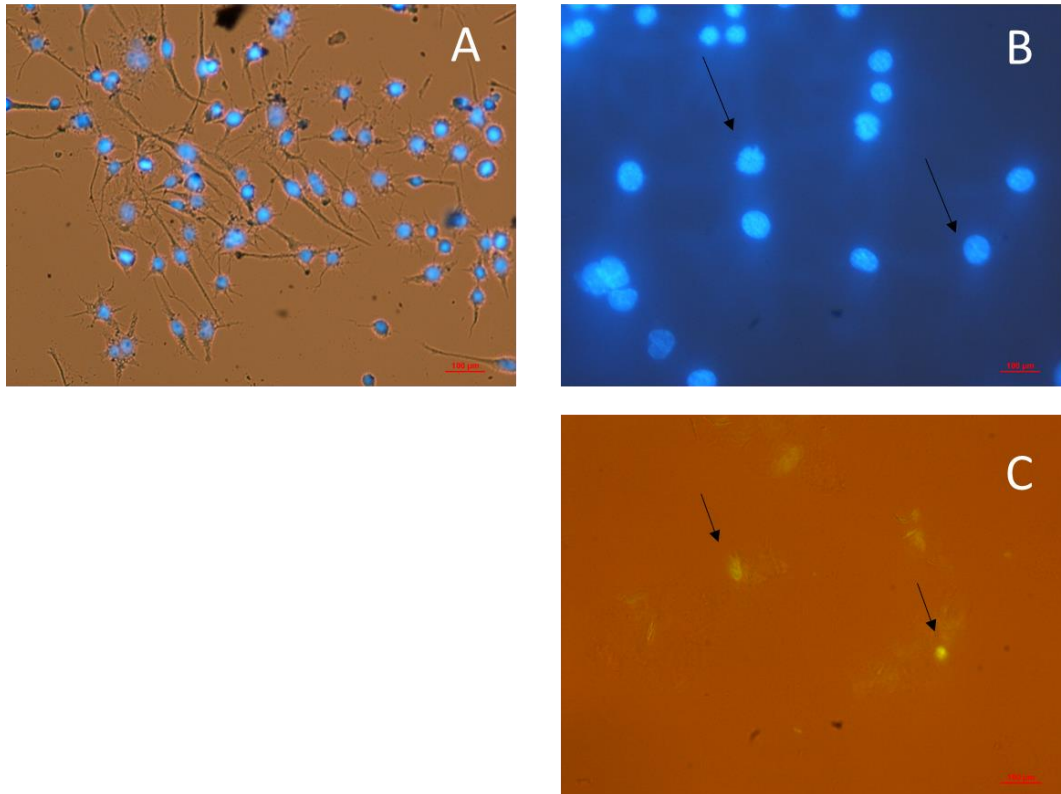


Figure 23 - Uptake images after 3 hours of incubation with liposomes. A - Control; B Nuclei Staining with DAPI; C - MLV 7:3 Liposomes localization. Scale bar **100 µM**.

The main reason, why it is not possible to see any liposomes in the majority of the samples evaluated is that all the experiments were done based on indomethacin concentrations instead of lipid concentration. Due to this, the amount of liposomes might not have been enough for the sufficient contrast of green fluorescent signal.

5. *In vitro* Permeation

Figure 24 is representative of the permeation patterns of liposomes. It is possible to notice that the highest release profiles were found for formulations containing SA, mainly MLV SA (1%). The higher values of skin permeation for all the time points were found for MLV SA, followed by LUV SA, MLV 7:3 and last LUV 7:3 (0.4%). Observing Figure 24, it is possible to observe that it did not occur burst release, which means that the release of indomethacin to the donor site was not quick. Also, it is noticeable that MLVs have a higher permeation than LUVs.

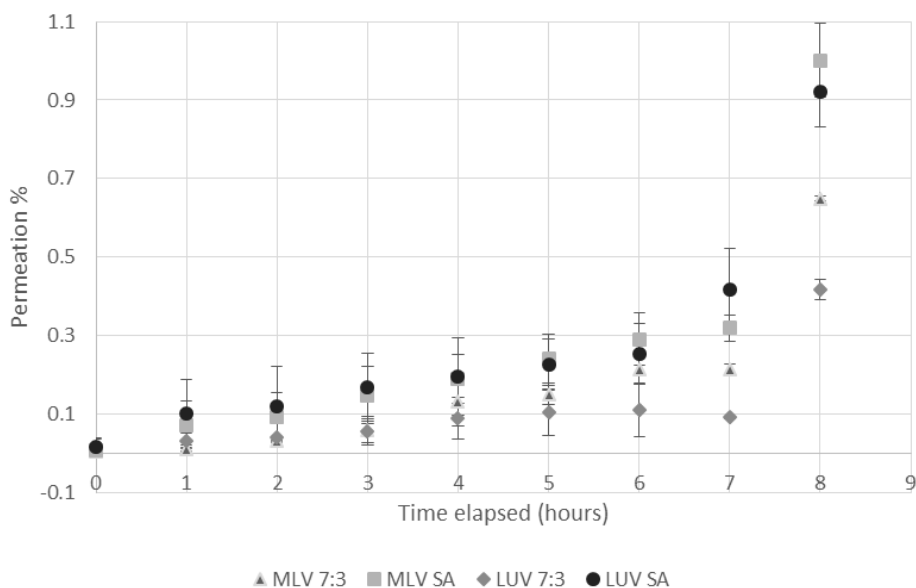


Figure 24 - Permeation profiles of liposomal formulation over 8 hours. Mean and SD of two independent assays.

Helleberg et al. described that the peak plasma concentration of indomethacin ranged from 2 - 3 $\mu\text{g}/\text{mL}$ of indomethacin. [144] In this assay, after 8 hours, the amount of indomethacin that crossed the skin is resumed in table 13. It is possible to conclude, that the amount of indomethacin that successfully crossed the skin is lower than the plasma concentration of indomethacin. Nonetheless this can be explained by the fact that the area used to evaluate the permeability was very small (0.64 cm^2), and the volume applied was only of $500 \mu\text{L}$. Thereby, if this area and the volume were increased the liposomes passage through the skin and as a consequence the indomethacin concentration should be increased.

However, in order to increase the amount of indomethacin that actually penetrated the skin a technological strategy could be employed. This strategy consists in the production of a hydrogel that enhances the penetration through the skin.

Table 13 - Indomethacin concentrations after 8 hours of permeation.

Indomethacin ($\mu\text{g}/\text{mL}$)	
MLV 7:3	0.225144
MLV SA	0.206325
LUV 7:3	0.137607
LUV SA	0.177836

- This page was purposely left in blank -

Chapter 7 - Conclusions

pH responsive liposomes containing indomethacin were successfully produced during this work. In fact, several formulations were produced and characterized. LUVs presented higher stability when compared to MLVs. Also, the amount of indomethacin loaded in the liposomes was almost the same and this difference was not statistical significant.

The release patterns of the formulations evaluated did not present any differences at the same pH, following the same pattern. However, when comparing both pHs it is possible to notice that at pH 7.4 the amount of indomethacin released is higher than at pH 5. One of the explanations for this occurrence is the inability of indomethacin to solubilize at this pH value.

Regarding liposomes interaction with cells it was possible to found that all the formulations affected macrophage more than fibroblasts, being MLV 7:3 the formulations with higher cytotoxicity. Also, Raw 264.7 morphology was highly influenced by the addition of liposomes.

Taking in account all the work performed in this dissertation, in my opinion, the best formulations for the following studies are MLV 7:3 and MLV SA. These formulations present controlled sized without extrusion, constant values of EE and LC and are easier to prepare. Also, they seem to affect macrophage and pass through the skin at a higher rate which are desirable characteristics.

- This page was purposely left in blank -

Chapter 8 - Future Remarks

The liposomal formulations made during this period present some interesting characteristics. However, there are always several assays that can be re-done and others that could be add for the improvement of the work. They comprise:

1. Liposomal formulations optimization:

- a. Stability enhancement due to liophilization;

2. *In Vitro* Assays

- a. Cytotoxicity evaluation using lactose dehydrogenase (LDH) cytotoxicity assay for the two cell lines tested (Raw 264.7 and L929);
- b. Repeat the assays with L929 to achieve statistical significance;
- c. Perform uptake assays with higher sensitivity for both cell lines, for example flow cytometry;
- d. Determination of macrophage inflammatory state using biomarkers for TNF α , IL-1 and IL-6;
- e. Quantification of indomethacin released in the cells by high-performance liquid chromatography.

3. *In Vivo* Assays

- a. Evaluation of the inflammation process in an animal model, mice, after contact with liposomes.

- This page was purposely left in blank -

References

1. SYMMONS, D.P.M., et al., *THE INCIDENCE OF RHEUMATOID ARTHRITIS IN THE UNITED KINGDOM: RESULTS FROM THE NORFOLK ARTHRITIS REGISTER*. *Rheumatology*, 1994. **33**(8): p. 735-739.
2. Sangha, O., *Epidemiology of rheumatic diseases*. *Rheumatology*, 2000. **39**(suppl 2): p. 3-12.
3. McDuffie, F.C., *Morbidity impact of rheumatoid arthritis on society*. *American Journal of Medicine*, 1985. **78**(1 A): p. 1-5.
4. Gaffo, A., K.G. Saag, and J.R. Curtis, *Treatment of rheumatoid arthritis*. *American Journal of Health-System Pharmacy*, 2006. **63**(24): p. 2451-2465.
5. Goodson, N.J., et al., *Mortality in early inflammatory polyarthritis: Cardiovascular mortality is increased in seropositive patients*. *Arthritis & Rheumatism*, 2002. **46**(8): p. 2010-2019.
6. Janssens, H.J.E.M., et al., *The Dutch College of General Practitioners guidelines on arthritis*. *NHG-standaard arthritis*, 2009. **52**(9): p. 439-454.
7. Olsen, N.J. and C.M. Stein, *New Drugs for Rheumatoid Arthritis*. *New England Journal of Medicine*, 2004. **350**(21): p. 2167-2179+2226.
8. Staff, H., *Healthy Joint vs. Damaged Joint*. 2004, Nucleus Communications, Inc.
9. Metselaar, J.M. and G. Storm, *Liposomes in the treatment of inflammatory disorders*. *Expert Opinion on Drug Delivery*, 2005. **2**(3): p. 465-476.
10. Pham, C.T.N., *Nanotherapeutic approaches for the treatment of rheumatoid arthritis*. *Wiley Interdisciplinary Reviews: Nanomedicine and Nanobiotechnology*, 2011. **3**(6): p. 607-619.
11. Scott, I.C., et al., *Precipitating and perpetuating factors of rheumatoid arthritis immunopathology - linking the triad of genetic predisposition, environmental risk factors and autoimmunity to disease pathogenesis*. *Best Practice & Research Clinical Rheumatology*, 2011. **25**(4): p. 447-468.
12. Hill, J.A., et al., *Cutting edge: The conversion of arginine to citrulline allows for a high-affinity peptide interaction with the rheumatoid arthritis-associated HLA-DRB1*0401 MHC class II molecule*. *Journal of Immunology*, 2003. **171**(2): p. 538-541.
13. Nepom, G.T., *Major histocompatibility complex-directed susceptibility to rheumatoid arthritis*. 1998. p. 315-332.
14. Bottini, N., et al., *Role of PTPN22 in type 1 diabetes and other autoimmune diseases*. *Seminars in Immunology*, 2006. **18**(4): p. 207-213.
15. Suzuki, A., et al., *Functional haplotypes of PADI4, encoding citrullinating enzyme peptidylarginine deiminase 4, are associated with rheumatoid arthritis*. *Nature Genetics*, 2003. **34**(4): p. 395-402.
16. *Infection and rheumatoid arthritis: Guilt by association?* *Journal of Rheumatology*, 2000. **27**(3): p. 564-566.
17. Symmons, D.P.M., et al., *Blood transfusion, smoking, and obesity as risk factors for the development of rheumatoid arthritis: Results from a primary care-based incident case-control study in Norfolk, England*. *Arthritis and Rheumatism*, 1997. **40**(11): p. 1955-1961.

18. Voigt, L.F., et al., *Smoking, obesity, alcohol consumption, and the risk of rheumatoid arthritis*. *Epidemiology*, 1994. **5**(5): p. 525-532.
19. Tarner, I.H., et al., *The different stages of synovitis: Acute vs chronic, early vs late and non-erosive vs erosive*. *Best Practice and Research: Clinical Rheumatology*, 2005. **19**(1): p. 19-35.
20. Firestein, G.S., *Invasive fibroblast-like synoviocytes in rheumatoid arthritis: Passive responders or transformed aggressors?* *Arthritis and Rheumatism*, 1996. **39**(11): p. 1781-1790.
21. Koch, A.E., *Angiogenesis as a target in rheumatoid arthritis*. *Annals of the Rheumatic Diseases*, 2003. **62**(SUPPL. 2): p. 60-67.
22. Keffer, J., et al., *Transgenic mice expressing human tumour necrosis factor: A predictive genetic model of arthritis*. *EMBO Journal*, 1991. **10**(13): p. 4025-4031.
23. Makkar, G.S. *Rheumatoid arthritis (RA) Overview*. 2010 [cited 2013 25th July 2013]; Available from: <http://askdrmakkar.com/rheumatoid.htm>.
24. Hochberg, M.C., et al., *The American College of Rheumatology 1991 revised criteria for the classification of global functional status in rheumatoid arthritis*. *Arthritis and Rheumatism*, 1992. **35**(5): p. 498-502.
25. Turesson, C., et al., *Extra-articular disease manifestations in rheumatoid arthritis: Incidence trends and risk factors over 46 years*. *Annals of the Rheumatic Diseases*, 2003. **62**(8): p. 722-727.
26. Aletaha, D., et al., *2010 Rheumatoid arthritis classification criteria: An American College of Rheumatology/European League Against Rheumatism collaborative initiative*. *Annals of the Rheumatic Diseases*, 2010. **69**(9): p. 1580-1588.
27. Kaarela, K., J. Kauppi, and M. Kauppi, *The 2010 ACR/EULAR classification criteria for rheumatoid arthritis in the Heinola inception cohort—diagnoses confirmed by long-term follow-up*. *Clinical Rheumatology*, 2012. **31**(3): p. 547-551.
28. Kaarela, K., M.J. Kauppi, and K.E.S. Lehtinen, *The value of the ACR 1987 criteria in very early rheumatoid arthritis*. *Scandinavian Journal of Rheumatology*, 1995. **24**(5): p. 279-281.
29. Shmerling, R.H. and T.L. Delbanco, *How useful is the rheumatoid factor? An analysis of sensitivity, specificity, and predictive value*. *Archives of Internal Medicine*, 1992. **152**(12): p. 2417-2420.
30. Wakefield, R.J., et al., *Noninvasive techniques for assessing skeletal changes in inflammatory arthritis: Imaging technique*. *Current Opinion in Rheumatology*, 2004. **16**(4): p. 435-442.
31. Junior, W.C.T., R. Rolim, and A.M. Kakehasi, *Magnetic resonance imaging in rheumatoid arthritis*. *Revista Brasileira de Reumatologia*, 2011. **51**(6): p. 629-641.
32. Mitragotri, S. and J.W. Yoo, *Designing micro- and nano-particles for treating rheumatoid arthritis*. *Archives of Pharmacal Research*, 2011. **34**(11): p. 1887-1897.
33. Van Den Hoven, J.M., et al., *Liposomal drug formulations in the treatment of rheumatoid arthritis*. *Molecular Pharmaceutics*, 2011. **8**(4): p. 1002-1015.
34. O'Dell, J.R., *Therapeutic strategies for rheumatoid arthritis*. *New England Journal of Medicine*, 2004. **350**(25): p. 2591-2602+2630.
35. Newsome, G., *Guidelines for the management of rheumatoid arthritis: 2002 update*. *Journal of the American Academy of Nurse Practitioners*, 2002. **14**(10): p. 432-437.
36. Simon, L.S., *DMARDs in the treatment of rheumatoid arthritis: Current agents and future developments*. *International Journal of Clinical Practice*, 2000. **54**(4): p. 243-249.
37. Russell, J.K., Anthony, *Systemic Glucocorticoid Treatment in Rheumatoid Arthritis - A Debate: EDITORIAL REVIEW*. *Scandinavian Journal of Rheumatology*, 1998. **27**(4): p. 247-251.
38. Zöllner, E.W., *Hypothalamic-pituitary-adrenal axis suppression in asthmatic children on inhaled corticosteroids (Part 2) - the risk as determined by gold standard adrenal function tests: A systematic review*. *Pediatric Allergy and Immunology*, 2007. **18**(6): p. 469-474.
39. Mahachoklertwattana, P., et al., *Suppression of adrenal function in children with acute lymphoblastic leukemia following induction therapy with corticosteroid and other cytotoxic agents*. *The Journal of pediatrics*, 2004. **144**(6): p. 736-740.

40. Saag, K., *Glucocorticoid use in rheumatoid arthritis*. Current Rheumatology Reports, 2002. 4(3): p. 218-225.
41. O'Dell, J.R., *Therapeutic Strategies for Rheumatoid Arthritis*. New England Journal of Medicine, 2004. 350(25): p. 2591-2602.
42. Madhok, M.M.C.H.A.C.R., *Recent Advances in the management of rheumatoid Arthritis*. Royal College of Physicians of Edinburgh, 2005. 35: p. 239-245.
43. Vane, J.R. and R.M. Botting, *The mechanism of action of aspirin*. Thrombosis Research, 2003. 110(5-6): p. 255-258.
44. Vane, J.R. and R.M. Botting, *Mechanism of action of nonsteroidal anti-inflammatory drugs*. American Journal of Medicine, 1998. 104(3 A): p. 2S-8S.
45. Vane, J.R., *The fight against rheumatism: From willow bark to COX-1 sparing drugs*. Journal of Physiology and Pharmacology, 2000. 51(4): p. 573-586.
46. Praveen Rao, P.N. and E.E. Knaus, *Evolution of nonsteroidal anti-inflammatory drugs (NSAIDs): Cyclooxygenase (COX) inhibition and beyond*. Journal of Pharmacy and Pharmaceutical Sciences, 2008. 11(2): p. 81s-110s.
47. Dugowson, C.E. and P. Gnanashanmugam, *Nonsteroidal Anti-Inflammatory Drugs*. Physical Medicine and Rehabilitation Clinics of North America, 2006. 17(2): p. 347-354.
48. FitzGerald, G.A., *COX-2 and beyond: Approaches to prostaglandin inhibition in human disease*. Nature Reviews Drug Discovery, 2003. 2(11): p. 879-890.
49. Conaghan, P.G., *A turbulent decade for NSAIDs: Update on current concepts of classification, epidemiology, comparative efficacy, and toxicity*. Rheumatology International, 2012. 32(6): p. 1491-1502.
50. Day, R.O., G.G. Graham, and K.M. Williams, *Pharmacokinetics of non-steroidal anti-inflammatory drugs*. Bailliere's Clinical Rheumatology, 1988. 2(2): p. 363-393.
51. Silverstein, F.E., et al., *Misoprostol Reduces Serious Gastrointestinal Complications in Patients with Rheumatoid Arthritis Receiving Nonsteroidal Anti-Inflammatory Drugs A Randomized, Double-Blind, Placebo-Controlled Trial*. Annals of Internal Medicine, 1995. 123(4): p. 241-249.
52. Hawkey, C.J., *Nonsteroidal anti-inflammatory drug gastropathy*. Gastroenterology, 2000. 119(2): p. 521-535.
53. Scheiman, J.M., *The impact of nonsteroidal anti-inflammatory drug-induced gastropathy*. The American journal of managed care, 2001. 7(1 Suppl): p. S10-4.
54. J.R. Vane, J.B., R.M. Botting, *Improved Nonsteroidal Anti Inflammatory Drugs-COX-2 Enzyme Inhibitors*, ed. K.A. Publishers. 1996.
55. Vane, J., *Towards a better aspirin*. Vol. 367. 1994. 215-6.
56. Singh, G., et al., *Celecoxib Versus Naproxen and Diclofenac in Osteoarthritis Patients: SUCCESS-I Study*. The American journal of medicine, 2006. 119(3): p. 255-266.
57. Bombardier, C., et al., *Comparison of Upper Gastrointestinal Toxicity of Rofecoxib and Naproxen in Patients with Rheumatoid Arthritis*. New England Journal of Medicine, 2000. 343(21): p. 1520-1528.
58. Laine, L., et al., *Assessment of upper gastrointestinal safety of etoricoxib and diclofenac in patients with osteoarthritis and rheumatoid arthritis in the Multinational Etoricoxib and Diclofenac Arthritis Long-term (MEDAL) programme: a randomised comparison*. The Lancet. 369(9560): p. 465-473.
59. Schnitzer, T.J., et al., *Comparison of lumiracoxib with naproxen and ibuprofen in the Therapeutic Arthritis Research and Gastrointestinal Event Trial (TARGET), reduction in ulcer complications: randomised controlled trial*. The Lancet. 364(9435): p. 665-674.
60. Silverstein Fe, F.G.G.J.L. and et al., *Gastrointestinal toxicity with celecoxib vs nonsteroidal anti-inflammatory drugs for osteoarthritis and rheumatoid arthritis: The class study: a randomized controlled trial*. JAMA: The Journal of the American Medical Association, 2000. 284(10): p. 1247-1255.
61. Gutthann, S.P., L.A. GarcíaRodríguez, and D.S. Raiford, *Individual Nonsteroidal Antiinflammatory Drugs and Other Risk Factors for Upper Gastrointestinal Bleeding and Perforation*. Epidemiology, 1997. 8(1): p. 18-24.

62. Huang, J.-Q., S. Sridhar, and R.H. Hunt, *Role of Helicobacter pylori infection and non-steroidal anti-inflammatory drugs in peptic-ulcer disease: a meta-analysis*. The Lancet, 2002. **359**(9300): p. 14-22.
63. Weil, J., et al., *Prophylactic aspirin and risk of peptic ulcer bleeding*. BMJ, 1995. **310**(6983): p. 827-830.
64. Ajani, U.A., et al., *Aspirin Use Among U.S. Adults: Behavioral Risk Factor Surveillance System*. American Journal of Preventive Medicine, 2006. **30**(1): p. 74-77.
65. Goldstein, J.L., et al., *The impact of low-dose aspirin on endoscopic gastric and duodenal ulcer rates in users of a non-selective non-steroidal anti-inflammatory drug or a cyclo-oxygenase-2-selective inhibitor*. Alimentary Pharmacology & Therapeutics, 2006. **23**(10): p. 1489-1498.
66. García Rodríguez, L.A. and L. Barreales Tolosa, *Risk of Upper Gastrointestinal Complications Among Users of Traditional NSAIDs and COXIBs in the General Population*. Gastroenterology, 2007. **132**(2): p. 498-506.
67. Aithal, G.P. and C.P. Day, *Nonsteroidal Anti-Inflammatory Drug-Induced Hepatotoxicity*. Clinics in Liver Disease, 2007. **11**(3): p. 563-575.
68. Teoh, N.C. and G.C. Farrell, *Hepatotoxicity associated with non-steroidal anti-inflammatory drugs*. Clinics in Liver Disease, 2003. **7**(2): p. 401-413.
69. Antman, E.M., et al., *Use of Nonsteroidal Antiinflammatory Drugs: An Update for Clinicians: A Scientific Statement From the American Heart Association*. Circulation, 2007. **115**(12): p. 1634-1642.
70. Chou, R., et al., *Drug Class Review on Cyclo-oxygenase (COX)-2 Inhibitors and Non-steroidal Anti-inflammatory Drugs (NSAIDs): Final Report Update 3*. 2006, Portland OR: Oregon Health & Science University, Portland, Oregon.
71. FitzGerald, G.A., *Coxibs and Cardiovascular Disease*. New England Journal of Medicine, 2004. **351**(17): p. 1709-1711.
72. Strand, V. and M.C. Hochberg, *The risk of cardiovascular thrombotic events with selective cyclooxygenase-2 inhibitors*. Arthritis Care & Research, 2002. **47**(4): p. 349-355.
73. Proksch, E., J.M. Brandner, and J.-M. Jensen, *The skin: an indispensable barrier*. Experimental Dermatology, 2008. **17**(12): p. 1063-1072.
74. Kanitakis, J., *Anatomy, histology and immunohistochemistry of normal human skin*. Eur J Dermatol, 2002. **12**(4): p. 390-9; quiz 400-1.
75. Venus, M., J. Waterman, and I. McNab, *Basic physiology of the skin*. Surgery (Medicine Publishing), 2010. **28**(10): p. 469-472.
76. Brodell, L.A. and K.S. Rosenthal, *Skin Structure and Function: The Body's Primary Defense Against Infection*. Infectious Diseases in Clinical Practice, 2008. **16**(2): p. 113-117 10.1097/IPC.0b013e3181660bf4.
77. El Maghraby, G.M., B.W. Barry, and A.C. Williams, *Liposomes and skin: from drug delivery to model membranes*. Eur J Pharm Sci, 2008. **34**(4-5): p. 203-22.
78. Archer, C.B., *Functions of the Skin*, in *Rook's Textbook of Dermatology*. 2008, Blackwell Publishing, Inc. p. 129-140.
79. Scheuplein, R.J., *Mechanism of percutaneous adsorption. I. Routes of penetration and the influence of solubility*. J Invest Dermatol, 1965. **45**(5): p. 334-46.
80. Baroli, B., *Penetration of nanoparticles and nanomaterials in the skin: fiction or reality?* J Pharm Sci, 2010. **99**(1): p. 21-50.
81. Jaganathan, H. and B. Godin, *Biocompatibility assessment of Si-based nano- and micro-particles*. Advanced Drug Delivery Reviews, 2012. **64**(15): p. 1800-1819.
82. Panyam, J. and V. Labhasetwar, *Biodegradable nanoparticles for drug and gene delivery to cells and tissue*. Advanced Drug Delivery Reviews, 2003. **55**(3): p. 329-347.
83. Galvin, P., et al., *Nanoparticle-based drug delivery: case studies for cancer and cardiovascular applications*. Cellular and Molecular Life Sciences, 2012. **69**(3): p. 389-404.
84. Butoescu, N., O. Jordan, and E. Doelker, *Intra-articular drug delivery systems for the treatment of rheumatic diseases: A review of the factors influencing their performance*. European Journal of Pharmaceutics and Biopharmaceutics, 2009. **73**(2): p. 205-218.

85. J. Hwang, K.R., J.C. Oliver T. Schlupe, *alpha-Methylprednisolone conjugated cyclodextrin polymer-based nanoparticles for rheumatoid arthritis therapy*. International Journal of Nanomedicine, 2008. **3**(3): p. 359-371
86. Niu, R., et al., *Preparation, characterization, and antitumor activity of paclitaxel-loaded folic acid modified and TAT peptide conjugated PEGylated polymeric liposomes*. Journal of Drug Targeting, 2010. **19**(5): p. 373-381.
87. ROULLIN, V.G., et al., *Optimised NSAIDs-loaded Biocompatible Nanoparticles*. 2011. 2011.
88. Higaki, M., et al., *Treatment of experimental arthritis with poly(D, L-lactic/glycolic acid) nanoparticles encapsulating betamethasone sodium phosphate*. Annals of the Rheumatic Diseases, 2005. **64**(8): p. 1132-1136.
89. Saikat Das, R.B., Jayesh Bellare, *Aspirin Loaded Albumin Nanoparticles by Coacervation: Implications in Drug Delivery*. Trends Biomater. Artif. Organs, Vol 18 (2), January 2005, 2008.
90. Koo, O., I. Rubinstein, and H. Önyüksel, *Actively Targeted Low-Dose Camptothecin as a Safe, Long-Acting, Disease-Modifying Nanomedicine for Rheumatoid Arthritis*. Pharmaceutical Research, 2011. **28**(4): p. 776-787.
91. Rubinstein, I. and G.L. Weinberg, *Nanomedicines for chronic non-infectious arthritis: The clinician's perspective*. Maturitas, 2012. **73**(1): p. 68-73.
92. Trif, M., et al., *Liposomes as Possible Carriers for Lactoferrin in the Local Treatment of Inflammatory Diseases*. Experimental Biology and Medicine, 2001. **226**(6): p. 559-564.
93. Bhardwaj, U. and D.J. Burgess, *Physicochemical properties of extruded and non-extruded liposomes containing the hydrophobic drug dexamethasone*. International Journal of Pharmaceutics, 2010. **388**(1-2): p. 181-189.
94. Storm, G. and D.J.A. Crommelin, *Liposomes: quo vadis?* Pharmaceutical Science & Technology Today, 1998. **1**(1): p. 19-31.
95. BERGER, et al., *Filter extrusion of liposomes using different devices : comparison of liposome size, encapsulation efficiency, and process characteristics*. Vol. 223. 2001, Amsterdam, PAYS-BAS: Elsevier.
96. Jousma, H., et al., *Characterization of liposomes. The influence of extrusion of multilamellar vesicles through polycarbonate membranes on particle size, particle size distribution and number of bilayers*. International Journal of Pharmaceutics, 1987. **35**(3): p. 263-274.
97. Vanniasinghe, A.S., V. Bender, and N. Manolios, *The Potential of Liposomal Drug Delivery for the Treatment of Inflammatory Arthritis*. Seminars in Arthritis and Rheumatism, 2009. **39**(3): p. 182-196.
98. Schnyder, A. and J. Huwyler, *Drug transport to brain with targeted liposomes*. NeuroRX, 2005. **2**(1): p. 99-107.
99. Frank, M.M., *The reticuloendothelial system and bloodstream clearance*. Vol. 122. 1993. 487-8.
100. Storm, G., et al., *Surface modification of nanoparticles to oppose uptake by the mononuclear phagocyte system*. Advanced Drug Delivery Reviews, 1995. **17**(1): p. 31-48.
101. Metselaar, J.M., et al., *Complete remission of experimental arthritis by joint targeting of glucocorticoids with long-circulating liposomes*. Arthritis & Rheumatism, 2003. **48**(7): p. 2059-2066.
102. Metselaar, J.M., et al., *Liposomal targeting of glucocorticoids to synovial lining cells strongly increases therapeutic benefit in collagen type II arthritis*. Ann Rheum Dis, 2004. **63**(4): p. 348-353.
103. Immordino, M.L., F. Dosio, and L. Cattel, *Stealth liposomes: review of the basic science, rationale, and clinical applications, existing and potential*. Int J Nanomedicine, 2006. **1**(3): p. 297-315.
104. Drummond, D.C., et al., *Optimizing Liposomes for Delivery of Chemotherapeutic Agents to Solid Tumors*. Pharmacological Reviews, 1999. **51**(4): p. 691-744.

105. Harrington, K.J., et al., *Pegylated Liposomes Have Potential as Vehicles for Intratumoral and Subcutaneous Drug Delivery*. *Clinical Cancer Research*, 2000. **6**(6): p. 2528-2537.
106. Lasic, D.D. and N.S. Templeton, *Liposomes in gene therapy*. *Advanced Drug Delivery Reviews*, 1996. **20**(2-3): p. 221-266.
107. Mahato, R.I., et al., *Physicochemical and disposition characteristics of antisense oligonucleotides complexed with glycosylated poly(l-lysine)*. *Biochemical Pharmacology*, 1997. **53**(6): p. 887-895.
108. Templeton, N., et al., *Improved DNA: liposome complexes for increased systemic delivery and gene expression*. *Nat Biotech*, 1997. **15**(7): p. 647-652.
109. Yotnda, P., et al., *Bilamellar cationic liposomes protect adenovectors from preexisting humoral immune responses*. *Molecular Therapy*, 2002. **5**(3): p. 233-241.
110. Low, P.S., W.A. Henne, and D.D. Doorneweerd, *Discovery and Development of Folic-Acid-Based Receptor Targeting for Imaging and Therapy of Cancer and Inflammatory Diseases*. *Accounts of Chemical Research*, 2007. **41**(1): p. 120-129.
111. Goren, D., et al., *Nuclear Delivery of Doxorubicin via Folate-targeted Liposomes with Bypass of Multidrug-resistance Efflux Pump*. *Clinical Cancer Research*, 2000. **6**(5): p. 1949-1957.
112. Lee, R.J. and P.S. Low, *Delivery of liposomes into cultured KB cells via folate receptor-mediated endocytosis*. *Journal of Biological Chemistry*, 1994. **269**(5): p. 3198-3204.
113. Kaasgaard, T., O.G. Mouritsen, and K. Jørgensen, *Screening effect of PEG on avidin binding to liposome surface receptors*. *International Journal of Pharmaceutics*, 2001. **214**(1-2): p. 63-65.
114. Maruyama, K., et al., *Targetability of novel immunoliposomes modified with amphipathic poly(ethylene glycol) s conjugated at their distal terminals to monoclonal antibodies*. *Biochimica et Biophysica Acta (BBA) - Biomembranes*, 1995. **1234**(1): p. 74-80.
115. Bendas, G., et al., *Targetability of novel immunoliposomes prepared by a new antibody conjugation technique*. *International Journal of Pharmaceutics*, 1999. **181**(1): p. 79-93.
116. Levick, J.R., *Hypoxia and acidosis in chronic inflammatory arthritis; relation to vascular supply and dynamic effusion pressure*. *J Rheumatol*, 1990. **17**(5): p. 579-82.
117. Vogel, K., et al., *Peptide-Mediated Release of Folate-Targeted Liposome Contents from Endosomal Compartments1*. *Journal of the American Chemical Society*, 1996. **118**(7): p. 1581-1586.
118. Düzgüneş, N. and S. Nir, *Mechanisms and kinetics of liposome-cell interactions*. *Advanced Drug Delivery Reviews*, 1999. **40**(1-2): p. 3-18.
119. Hafez, I.M., S. Ansell, and P.R. Cullis, *Tunable pH-sensitive liposomes composed of mixtures of cationic and anionic lipids*. *Biophys J*, 2000. **79**(3): p. 1438-46.
120. Obata, Y., S. Tajima, and S. Takeoka, *Evaluation of pH-responsive liposomes containing amino acid-based zwitterionic lipids for improving intracellular drug delivery in vitro and in vivo*. *J Control Release*, 2010. **142**(2): p. 267-76.
121. Slepishkin, V.A., et al., *Sterically stabilized pH-sensitive liposomes. Intracellular delivery of aqueous contents and prolonged circulation in vivo*. *J Biol Chem*, 1997. **272**(4): p. 2382-8.
122. Torchilin, V., *Tumor delivery of macromolecular drugs based on the EPR effect*. *Adv Drug Deliv Rev*, 2011. **63**(3): p. 131-5.
123. Servier, *Powerpoint image bank*. 2012, LES LABORATOIRES SERVIER.
124. Lopes, S.C.d.A., et al., *Liposomes as Carriers of Anticancer Drugs*. *Cancer Treatment - Conventional and Innovative Approaches*. 2013.
125. Hart, F. and P. Boardman, *Indomethacin: a new non-steroid anti-inflammatory agent*. *British medical journal*, 1963.
126. J.G Hardman, L.E.L., P.B. Molinoff, R.W. Ruddon, A.G. Goodman, *Goodman and Gilman's The Pharmacological Basis of Therapeutics*. 1996, New York: McGraw-Hill.
127. Reference, P.D. *PDR.NET*. 2013; Available from: <http://www.pdr.net/drug-summary/indomethacin-capsules?druglabelid=1974>.

128. Sartor, M., *Dynamic light scattering*. University of California-San Diego. http://physics.ucsd.edu/neurophysics/courses/physics_173_273/dynamic_light_scattering_03.pdf, 2003.
129. Ltd, M.I., *Zetasizer Nano Series User Manual*. 2003, 2004.
130. Papahadjopoulos, D., et al., *Phase transitions in phospholipid vesicles. Fluorescence polarization and permeability measurements concerning the effect of temperature and cholesterol*. *Biochim Biophys Acta*, 1973. **311**(3): p. 330-48.
131. Michel, N., et al., *Determination of phase transition temperatures of lipids by light scattering*. *Chemistry and Physics of Lipids*, 2006. **139**(1): p. 11-19.
132. Marassi, R. and F. Nobili, *MEASUREMENT METHODS | Structural and Chemical Properties: Transmission Electron Microscopy*, in *Encyclopedia of Electrochemical Power Sources*, G. Editor-in-Chief: Jürgen, Editor. 2009, Elsevier: Amsterdam. p. 769-789.
133. Barzegar-Jalali, M., et al., *Kinetic analysis of drug release from nanoparticles*. *J Pharm Pharm Sci*, 2008. **11**(1): p. 167-77.
134. Hartley, J., et al., *Expression of infectious murine leukemia viruses by RAW264.7 cells, a potential complication for studies with a widely used mouse macrophage cell line*. *Retrovirology*, 2008. **5**(1): p. 1-6.
135. Hansen, J. and P. Bross, *A cellular viability assay to monitor drug toxicity*. *Methods Mol Biol*, 2010. **648**: p. 303-11.
136. Sylvester, P.W., *Optimization of the tetrazolium dye (MTT) colorimetric assay for cellular growth and viability*. *Methods Mol Biol*, 2011. **716**: p. 157-68.
137. Haldar, S. and A. Chattopadhyay, *Application of NBD-Labeled Lipids in Membrane and Cell Biology*, in *Fluorescent Methods to Study Biological Membranes*, Y. Mély and G. Duportail, Editors. 2013, Springer Berlin Heidelberg. p. 37-50.
138. Contri, R., et al., *Transport of Substances and Nanoparticles across the Skin and in Vitro Models to Evaluate Skin Permeation and/or Penetration*, in *Nanocosmetics and Nanomedicines*, R. Beck, S. Guterres, and A. Pohlmann, Editors. 2011, Springer Berlin Heidelberg. p. 3-35.
139. Meyer, W., R. Schwarz, and K. Neurand, *The skin of domestic mammals as a model for the human skin, with special reference to the domestic pig*. *Curr Probl Dermatol*, 1978. **7**: p. 39-52.
140. Colombo, P., et al., *5.12 - Biological In Vitro Models for Absorption by Nonoral Routes*, in *Comprehensive Medicinal Chemistry II*, B.T. Editors-in-Chief: John and J.T. David, Editors. 2007, Elsevier: Oxford. p. 279-299.
141. Lasic, D.D., *Liposomes: from physics to applications*. 1993: Elsevier.
142. Srinath, P., S.P. Vyas, and P.V. Diwan, *Preparation and pharmacodynamic evaluation of liposomes of indomethacin*. *Drug Dev Ind Pharm*, 2000. **26**(3): p. 313-21.
143. Huth, U.S., R. Schubert, and R. Peschka-Suss, *Investigating the uptake and intracellular fate of pH-sensitive liposomes by flow cytometry and spectral bio-imaging*. *J Control Release*, 2006. **110**(3): p. 490-504.

Appendix

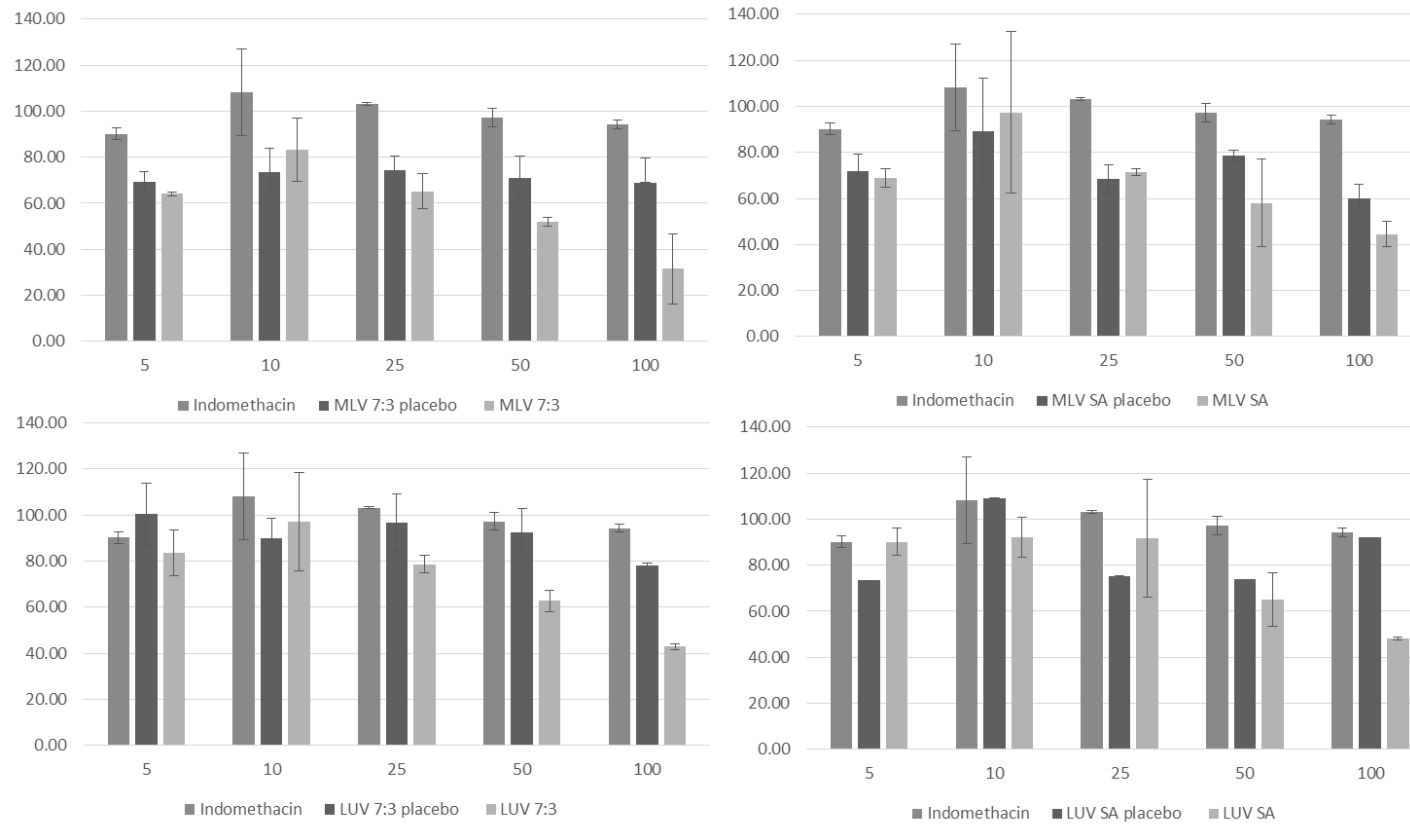


Figure 25 - Raw 264.7 viability after 24 hours of incubation with different liposome concentration, mean and standard deviation of two independent assays with 5 replica each.

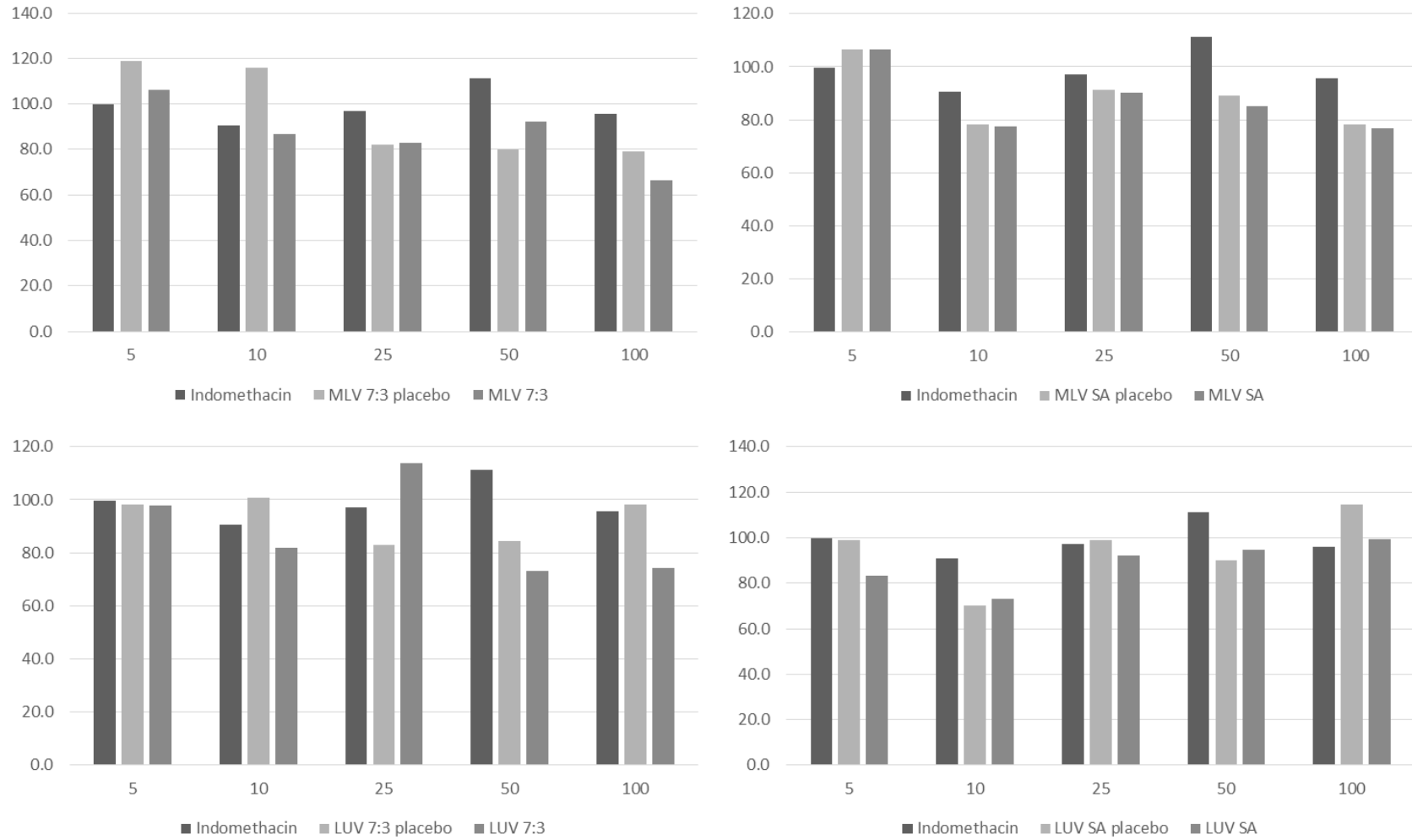


Figure 26 - L929 viability after 24 hours of incubation with different liposome concentration, mean and standard deviation 5 replica.

